Extreme high temperatures and adaptation by social dynamics: Theory and Evidence from China

Shi, Xiangyu and Gong, Jiaowei and Zhang, Xin and Wang, Chang

June 2024

Extreme high temperatures and adaptation by social dynamics: Theory and Evidence from China

Jiaowei Gong* Xiangyu Shi† Chang Wang‡ Xin Zhang§

July 1, 2024

Abstract

Using a novel city-level high-frequency panel data set of social and public events in Chinese cities, we document that extreme high temperatures significantly reshape social dynamics. Extreme high temperatures lead to an increase in social cooperation, and the effects are more salient when productivity is lower and labor is more intensively used. This implies extreme high temperatures boost the relative returns of cooperation given lowered productivity. Our estimates and quantitative model suggest that the human race adapts to global warming by reshaping its social dynamics: adaptation via social dynamics offsets about one-third of the negative impacts of extreme high temperatures on the economy.

JEL Classification: D71; D74; D9; O13; Q54; Q56

Keywords: Social dynamics; Public events; Social cooperation; Protest; Temperatures; Climate change; China

*Harvard University. Email: jiaowei_gong@hsph.harvard.edu

†Corresponding author. Department of Economics, Yale University. Email:xiangyu.shi@yale.edu

‡University of Michigan. Email: cwclaire@umich.edu

§Corresponding author. School of Statistics, Beijing Normal University. Email: xin.zhang614@bnu.edu.cn

1 Introduction

Social dynamics, defined and measured as the occurrence of social and public events in our paper, is a fundamental factor for economic development and societal welfare.[1] The existing literature in economics and sociology emphasizes the role of social networks, social media, and economic institutions in shaping social dynamics (Shiller et al., 1984; Abel et al., 2002; Olken, 2009; Marchand et al., 2021), but is almost silent regarding the role of environmental factors. In this paper, we are among the first to examine the effects of extreme high temperatures on social dynamics or the incidence of social and public events—in particular, cooperation in China—using a novel high-frequency data set.[2] In our case, cooperation is a means to create new economic opportunities, thus maintaining social and economic resilience in the face of climate stresses. Our results reveal the response of social dynamics to the current trend of global warming, a highly popular topic in academia and the policy realm.

We propose a conceptual framework and a simple theoretical model of collective actions (in Appendix B[3]) to guide our empirical analysis. The framework and the model exploit the nature that social cooperation is collective action that needs complementary efforts from all participants and the fact that extreme high temperatures increase the relative return of participation. Since productivity is lower under extreme high temperatures, people may turn to collaborative productivity-enhancing actions to compensate for the loss. In the case of social cooperation, the economy and society may find it profitable to engage in cooperation to create new economic opportunities to offset the negative effects of high temperature. Therefore, the framework and the model predict that extreme high temperatures increase the number of cooperation.

We start the empirical analysis with Poisson regressions, where the dependent variable is the counts of social cooperation, and the independent variables are the number of days in various temperature bins. We find that extreme high temperatures significantly increase social cooperation. One extra day with the temperature in the bin of T$>$ 32°C relative to the reference bin raises the average number of cooperation events by 1.76%.[4].

Several things are worth mentioning here: (1) We follow the tradition of the literature and treat the temperature fluctuation as exogenous variations, conditional on weather controls and fixed effects. Therefore, the same as the existing literature, we do not delve deep to deal with the potential endogeneity of temperatures. (2) We use Poisson regressions and the actual counts of public events as the dependent variables since the recent literature argues that using log transformations may yield significant bias (Chen and Roth, 2023). However, as robustness checks, we also employ an OLS estimation, using log

[1] In the sociology literature, social dynamics refers to the behavior of groups and the interactions of individual group members, and complex social behaviors among humans. We use the occurrence of social cooperation and protests to measure social dynamics.

[2] Social dynamics also include protests, which are negative public events. We also find a significant effect of extreme high temperatures on protests, though the results are less consistent.

[3] The models in Appendix B and Section 6.1 play different roles. The model in Appendix B rationalizes theoretical predictions in the conceptual framework, whereas the model in Section 6.1 builds a framework for quantitative analysis.

[4] Alternatively, as a robustness check, increasing cooling degree days by one day raises the expected count of cooperation by 0.1%.

transformations as the dependent variable. The results are still robust. (3) Although we have daily information on public events, we use a balanced city-year-month panel data set for analysis, mainly because the date of the public events may not be fully exact. For instance, it is reasonable to presume that cooperation plans are negotiated during a certain week but not on a certain day, so that it is not feasible to pinpoint the exact date. With the monthly dataset, the fuzziness of the dates may still be a concern if the events occur during the first or last days of each month. We therefore exclude such days from our sample as a robustness check. (4) It is possible that the approximate date of cooperation is determined before the actual date of occurrence. Therefore, we use a data set aggregated at coarser levels—semi-year- and year-levels—in which the planned date and the occurrence date are more likely to fall into the same time interval, and the results are still robust. We also find that extreme high temperatures have cumulative effects and lagged effects that suggest future impacts of hot days. (5) The results are not sensitive to controlling for different sets of fixed effects or control variables and are also not sensitive to different ways of clustering standard errors. (6) We use the number of days in different temperature bins as the main independent variables to capture the nonlinearity of the temperature effects, but our results are also robust to different temperature measures.

We then examine the underlying mechanisms and heterogeneity. Using interaction term regressions, we find that the positive effects of extreme high temperatures on cooperation are more salient when the city relies more heavily on labor-intensive industrial sectors and when the productivity of industrial sectors is lower. Such a result is consistent with our conceptual framework and theoretical model where the magnitude of the responses to extreme high temperatures depends on the opportunity cost parameter of engaging in public events. We also find regional spillover effects of extreme high temperatures, highlighting that inter-regional cooperation and coordination are needed in response to global warming.[5] Finally, we find temporal accumulative effects, which suggest that extreme high temperatures may have profound and enduring effects on social dynamics. Moreover, since cooperation may be facilitated before the actual occurrence date, the significance of the cumulative effects also indicates that extreme high temperatures indeed cause more cooperation (in the future).

We finally assess the economic implications of the response of social dynamics using both reduced-form estimates and a quantitative model. We find that cooperation has significant positive impacts on economic outputs, despite that extreme high temperatures and global warming reduce economic outputs. A back-of-the-envelope calculation using reduced-form estimates suggests that human adaptation by social cooperation mitigates the negative economic impacts of global warming by 34.6%. We also build an endogenous growth model with climate change and social dynamics and conduct quantitative analysis, which yields similar results. Therefore, our reduced-form empirical and quantitative analyses suggest that the human race adapts to the long-run trend of temperature rise by reshaping social dynamics. We also find that subsidizing cooperation is an effective way to combat global warming via the response of social dynamics. For example, subsidizing cooperation by 5% raises the equilibrium growth rate of the economy by 1.679%. Such results provide a guidance for a cost-benefit analysis for policymakers.

Our paper speaks to two strands of the literature. First, our paper contributes to the literature

[5]The results can be found in Table 8.

on the determinants of social dynamics, or social and public events. There are several recent papers on protests in China (Cantoni et al., 2019; Bursztyn et al., 2021; Cantoni et al., 2023), and other countries (Wallace et al., 2014). More relatedly, two recent papers discuss the effects of environmental factors on protests (Huang and Li, 2023; Li and Meng, 2023). However, there are few papers that empirically examine the determinants of social cooperation. We contribute to the literature by documenting how negative external shocks reshape the pattern of social cooperation and find that the incidence of social cooperation increases with extreme high temperatures.

Second, more broadly, our findings also contribute to the consequences and implications of extreme temperatures and global warming. Extreme temperatures can hinder economic development (Dell et al., 2009; Dell et al., 2012; Dell et al., 2014; Shi and Zhang, 2023), raise the mortality rate (Deschênes and Greenstone, 2011; Barreca et al., 2016; Yu et al., 2019), and increase the risk of mental illness (Obradovich et al., 2018; Mullins and White, 2019). In response to these effects, the human race is adaptive in terms of agricultural production (Deschênes and Greenstone, 2007), reorganizing firms (Zhang et al., 2018; Shi and Zhang, 2023), and reinvesting in human capital (Shah and Steinberg, 2017). Our paper provides an important implication that the response of social dynamics is a crucial means by which the human race is adapting to global warming and offsets its negative impacts. On the methodology side, apart from regression analysis as done in previous literature, we construct a novel endogenous growth model integrating elements of climate factors and adaptation to generate predictions, structurally estimate parameters, and conduct counterfactual analysis. We are among the first to quantitatively estimate the magnitude of adaptation compared to productivity loss due to extreme high temperatures, highlighting the pivotal role of social dynamics in maintaining economic resilience.

The remainder of this paper is organized as follows. Section 2 discusses the background and develops the hypotheses. Section 3 describes the data. Section 4 introduces the empirical strategies. Section 5 presents and discusses the empirical results. Section 6 conducts a set of macroeconomic analyses that feature an endogenous growth model, calibration, and counterfactual experiments. Finally, Section 7 concludes.

2 Conceptual Framework

2.1 Background

Social dynamics refers to the patterns of interaction, behavior, and relationships among individuals and groups within a society. As the canonical paper by Montroll (1978) shows, the rate of change in social evolutionary processes is considered constant, while the outbreak of public events causes deviation. Public events may serve as a catalyst for social dynamics by creating a platform for communication, expression, and mobilization. Cooperation, for example, helps mobilize groups toward a common goal. Public events of social cooperation are also considered social movements that would foster a sense of collective identity and a shared narrative or purpose (Polletta and Jasper, 2001). Given the above reasoning, we use the incidence of public events, in particular, social cooperation, as a measure of social dynamics.

During the last century, an increase in both average and extreme temperatures have caused a lot of concerns. The impacts of extreme temperatures extend beyond the realm of climate and have far-reaching consequences in various domains, particularly in health, income, and productivity (Deschênes and Greenstone, 2011; Zivin and Kahn, 2016; Auffhammer, 2018). However, little is known regarding the effects of extreme temperature on social dynamics.

Different ways are documented in the literature to adapt to the rising temperature and minimize its negative impacts. For example, in agriculture, expansion of irrigation and utilization of saved financial assets and crop stocks are found to be the effective adaptation channels (Cui and Tang, 2024; Wang et al., 2024). For households, effective adaptation methods mainly include using more energy (for air-conditioning, etc), while the introduction of health care programs would mitigate the temperature-health relationship (Deschênes and Greenstone, 2011; Banerjee and Maharaj, 2020; Hua et al., 2023). Workers also adapt to rising temperatures by working longer hours (LoPalo, 2023).

Social dynamics or social cooperation in response to global warming involves collective efforts at various levels of society to address and mitigate the impacts of climate change. These cooperative actions are crucial in fostering resilience, innovation, and adaptability. For example, communities may foster initiatives including forming groups to tackle local climate issues, such as planting trees, organizing recycling programs, and setting up community gardens. In addition, governments may involve citizens in policy-making through cooperative public consultations, hearings, and participatory budgeting for climate projects, and cooperative partnerships between governments, NGOs, businesses, and communities facilitate the development and implementation of comprehensive climate strategies.

2.2 Hypothesis Development

We formulate several hypotheses in a conceptual framework that can further be rationalized by a theoretical model in Appendix B. Our conceptual framework starts with the well-established premise in the literature that extreme high temperatures cause discomfort and hurt productivity.

Given a standard discrete choice framework in which individuals choose from engaging in routine jobs or outside options such as initiating social cooperation that creates new economic opportunities, extreme high temperatures reduce the opportunity costs of routine jobs as productivity is lowered during heat waves.[6] Thus, the relative returns of cooperation increases. Therefore, we have Hypothesis 1. This hypothesis is aligned with Prediction B1 in the theoretical model in Appendix B.

Hypothesis 1. *Higher temperatures foster cooperation.*

Next, we start to focus on comparative statics, i.e., in what situations the effects of extreme high temperatures are more salient. Following the above line of reasoning of opportunity costs and relative returns, the answer is obvious and self-explanatory: When the return of routine jobs is lower, extreme high temperatures will foster the engagement of outside options more, since rational decision-makers simply

[6]It is intuitive that high temperatures lead to human discomfort and reduce labor productivity. On the other hand, as Zhang et al. (2018) and Shi and Zhang (2023) argue, high temperatures also reduce capital productivity.

compare the costs and benefits of different alternatives and choose the best one. This is especially the case for regions with low productivity that is associated with a smaller opportunity cost[7]. As a result, we have the following Hypothesis 2, consistent with Prediction B2 in the theoretical model in Appendix B.

Hypothesis 2. *Higher temperatures foster cooperation more when the opportunity cost of the routine job is smaller or the return of cooperation is higher.*

3 Data

3.1 Public Event Data

We use the Global Data on Events, Location, and Tone (GDELT) database to compile a data set of city-level cooperation [8]. The definition of cooperation as per GDELT is provided in Table A1 and we further provide two case analyses of cooperation in Appendix A. The GDELT database is increasingly used in studies of social unrest (Barrett et al., 2022). The database applies textual analysis and machine learning methods to record salient characteristics (e.g., location, date, category, actor) of public events based on articles from a comprehensive set of global news resources. It is noteworthy that the date of cooperation mainly documents the date of signing cooperation agreements, which generally happens indoors and is thus less subject to the influence of extreme high temperatures.

Each event in the GDELT data set is classified under the Conflict and Mediation Events Observations (CAMEO) Event and verb codebook, where economic and technical cooperation, diplomatic cooperation (praise or endorse, defend verbally, rally support on behalf of, grant diplomatic recognition, apologize, forgive, sign a formal agreement) are three of the top twenty verbs that can be classified as. For cooperation events, we calculate the number of total cooperation events at the city level as the sum of material cooperation and diplomatic cooperation. Additionally, we recategorize three main sub-group cooperation: diplomatic cooperation, economic and technical cooperation (economic cooperation and intelligence or information cooperation), and law cooperation (judicial cooperation and military cooperation).[9] The definition of each category of cooperation is provided in Table A1. We provide two case analyses for cooperation in Appendix D.

Using this database, we compile a balanced city-year-month panel data set that covers 273 prefecture cities and three years from January 2013 to December 2015 with 121,825 cooperation events. Figure 1 (a) shows the time trends of public events, and Figure 1 (b) and (c) show the spatial distribution of public events. Descriptive statistics are shown in Table A2.

We use the data of 2013-2015 for the following reasons. Using the method proposed in Bai and Perron (1998) and Bai and Perron (2003), we find that there is a structural break in our public event data during 2015-2016. As a result, we use the pre-2015 sample that maintains internal structural consistency.

[7] In the empirical analysis, productivity is measured using TFP and labor productivity.

[8] `https://www.gdeltproject.org/`. The database is also used in Beraja et al. (2023).

[9] Economic and technical cooperation occupies the largest share of all cooperation events.

After 2015, social cooperation is dominantly initiated by the government due to the "one-belt-one-road" initiatives, contributing to a paradigm shift of the data. Moreover, the Chinese economy entered the phase of "new normal" in around 2015,[10] featuring a shift in the pattern of economic growth and policy-making and contributing to the structural break of the data. We use the sample period of pre-2015 which is consistent with the growth pattern during the past four decades after the economic reform in 1978. In addition, the period of 2013-2015 has a relatively larger variability of temperatures (about 1.7 times larger than that of the post-2015 period), which provides a better empirical testing ground to estimate the effects of temperatures on social dynamics. Finally, data before 2013 is aggregated at the annual level, and, thus, we can only use the post-2013 sample to obtain monthly, weekly, and daily variations.

We provide the scatter plots and the linear fit between (1) GDP growth and mean temperature and (2) cooperation and mean temperature. The results in Figure C3 show that there is a significant negative relationship for (1) and a significant positive relationship for (2). Such results are consistent with our main findings.

3.2 Temperatures and Weather Data

The data of temperatures and other weather covariates are obtained from the China National Meteorological Data Service Center.[11] The data set contains consecutive daily weather records of 824 monitoring stations along with their longitudes and latitudes in China.[12] The key variable for our analysis was the daily mean temperature. Other weather controls include precipitation, wind speed, and relative humidity.[13] We interpolate the data from the stations into a $0.1° \times 0.1°$ grid level using the inverse-distance weighting (IDW) method and extract the value of the measures based on the boundaries of each city from the gridded data. Interpolating the weather data from stations into the grid level enables us to match the weather data following the exact boundaries for each city, which can help ameliorate the concerns about potential measurement errors caused by the imprecise matching radius for some geographically large or small cities when using IDW method.[14] Following the general practice used in the latest literature (Deschênes and Greenstone, 2011), we calculate the number of days falling into each 4°C-wide bin by city-year-month. We also use other measures of temperatures as robustness checks. Table A2 presents some of the summary statistics. Figure C1 plots the time series of temperature fluctuations during 2013-2015.

[10] See the detailed policy description here: `https://english.www.gov.cn/china_economic_new_normal/`

[11] The dataset has been widely used in the recent literature when studying weather/climate change in China (for example, Agarwal et al., 2021; Zivin et al., 2020).

[12] Figure C2 (a) displays the distribution of the weather stations. As far as we know, the distribution of the monitoring stations in this data set is finer than that of the gridded temperature products, which are typically at the $0.5° \times 0.625°$ grid level.

[13] In the regression analysis, we control for them and their high-order polynomials.

[14] Figure C2 (b) illustrates the spatial distribution of the yearly mean temperature from 2013 to 2015 using the interpolating method.

3.3 Other Data

We use other data to construct interaction terms and prove the mechanisms proposed in our hypothesis. To measure productivity, we use the Annual Survey of Industrial Firms (ASIF) database. The ASIF data during 1998-2007 has all the information needed to calculate the total factor productivity (TFP) using OP, OP-ACF corrected, LP, and LP-ACF corrected methods, as well as labor productivity (Olley and Pakes, 1996; Levinsohn and Petrin, 2003; Ackerberg et al., 2015). We calculate the TFP and labor productivity at the firm level and then take the median of the TFP of all firms at the city level during the period of 1998-2007. Population and the share of the industrial sector are from the Chinese City Statistics Yearbooks. Education level is from Population Census data in 2010.

4 Empirical Strategy

4.1 Estimating the Effects of Temperatures on Social Dynamics

The main specification of the descriptive empirical analysis in this section takes the form of equation (1), which is obtained using a city-year-month panel data set and a Poisson Pseudo Maximum Likelihood (PPML) regression that follows the previous literature:

$$\log(E(y_{imt}|\Gamma_{imt})) = \sum_{group,group\neq 4} \beta_{group} D_{group,imt} + X_{imt}\delta + \lambda_{it} + \lambda_{mt}, \quad (1)$$

where y_{imt} is the outcome variable, including the count of cooperation, in the city i, year t, and month m, Γ_{imt} is a vector of conditioning variables on the right-hand side, $D_{group,imt}$ is the number of days that fall into each 4-degree temperature interval (T$\geq$ 32°C, 28°C$\leq$T$<$32°C, 24°C$\leq$T$<$28°C, 20°C$\leq$T$<$24°C, 16°C$\leq$T$<$20°C, 12°C$\leq$T$<$16°C, 8°C$\leq$T$<$12°C, 4°C$\leq$T$<$8°C, 0°C$\leq$T$<$4°C, $-$4°C$\leq$T$<$0°C, and T$<-$4°C), with the fourth group 20°C$\leq$T$<$24°C being excluded as the base group. The bins allow for a nonlinear relationship between temperatures and outcomes. X_{imt} is a vector of controls including precipitation, sunshine duration, and wind speed. λ_{it} is city-year fixed effects that absorb all variations at the city-year level;[15] λ_{mt} is year-month fixed effects. In some regressions, we also control for city-month fixed effects. We cluster standard errors in a two-way fashion at the city and year levels, to allow for cross-sectional and serial correlations of error terms. For robustness checks, we also control for province-year-season fixed effects, province-year-month fixed effects, and city-year-month linear time trends, and the results remain robust. We two-way cluster the standard errors at city and year level. The results are still robust to other ways of clustering.

Using equation 1, β_{group} are identified from the variations in temperatures within a city across years and months after adjusting for covariates and temporal shocks common to all the cities. Due to the unpredictability of temperature fluctuations, it is reasonable to follow the literature and presume

[15]Having controlled for the city-year fixed effects, we do not need to control for city-year variables such as GDP, population, etc.

that this variation is orthogonal to the unobserved determinants of social dynamics. Therefore, we use PPML and OLS regressions throughout this paper.

Next, we use alternative measures of high-temperature exposure. Specifically, we exploit equation (2) and a city-year-month panel data set:

$$\log(E(y_{imt}|\Gamma_{imt})) = \beta Temperature_{imt} + X_{imt}\delta + \lambda_{it} + \lambda_{mt}, \tag{2}$$

where $Temperature_{imt}$ is a measure of extreme high temperatures, and β is the parameter of interest. The rest of the equation is the same as that of equation (1). We construct the measure of extreme high temperatures in three ways. First, we calculate the cooling degree days, which quantify the average number of degrees by which the daily mean temperature exceeds 24°C, with values below 24°C assigned a value of 0. Second, to address the variability of climate across different regions, we determine the mean and standard deviation (SD) of daily temperatures from 1980 to 2010 for each city. Subsequently, we utilize the count of days where the daily mean temperature surpasses the mean plus two times the SD to assess extreme temperatures relative to historical norms. Third, we assess the duration of heat waves by calculating the consecutive days with daily mean temperatures exceeding 32°C.

4.2 Estimating the Effects of Social Dynamics on Socioeconomic Outcomes

To evaluate the effects of social dynamics or public events on socioeconomic outcomes, we employ the following OLS regression:

$$y_{it} = \alpha \log(PublicEvent_{it}) + \lambda_i + \lambda_t + u_{it}, \tag{3}$$

where y_{it} is the outcome in the city i and year t, $PublicEvent_{it}$ is the log cooperation, λ_i is the city fixed effects, λ_t is the year fixed effects, and u_{it} is the error term. We cluster the standard error at the city level. Note that due to the endogeneity of $\log(PublicEvent_{it})$, equation (3) cannot serve for causal estimation. We only use the estimates to conduct a back-of-the-envelope calculation of the impacts on the economy.

5 Empirical Results

In this section, we present the main empirical results, including the baseline results, mechanisms and heterogeneity analysis, robustness checks, and implications for the economy.

5.1 Baseline Results

We first estimate the effects of temperatures on the public events of cooperation using equation (1). The dependent variable is the untransformed count of cooperation events, and the estimation technique

is PPML. We report the results in Table 1. In columns (1) and (2), the dependent variable is the count of cooperation, and we control for different sets of fixed effects. The coefficients of T>32°C are both positive and statistically significant. For column (2), increasing the number of days in the temperature bin of T>32°C by one day relative to the reference bin leads to an increase of cooperation by 1.48 ($100\times(e^{1.47}$-1)%) on average.

Moreover, Figure 2 plots the regression coefficients of Table 1 column (2). It is also noteworthy that for the high-temperature bins, the bin of the highest temperature has the largest positive effect. For example, in column (1), the coefficient of T>32°C is 0.0507, and the coefficients of T$\in (28, 32]$°C and T$\in (24, 28]$°C are 0.0141 and 0.0105, respectively, and both are not statistically significant.

The results that extreme high temperatures increase the number of cooperation can be explained as follows. Extreme high temperatures change the relative return of participation in public events. Since productivity is lower under extreme high temperatures, people may turn to other activities that have a higher return. The economy and society may find it profitable to engage in cooperation that creates new economic opportunities to offset the negative effects of global warming. Thus, cooperation is a means by which society responds to potential challenges of climate change. Such arguments are consistent with Hypothesis 1 and Prediction B1.

Next, we control for alternative sets of controls and fixed effects and show that the results are still qualitatively robust. In Table 2, we control for higher-order polynomials of weather variables (up to fourth order), and the results are still qualitatively and quantitatively robust. In Table 3, we additionally control for province-year-month fixed effects and city-year-month linear trends, and the coefficient on T>32°C is statistically significant at at least 5% level. Therefore, in sum, our main results are robust to the inclusion of higher-order polynomial of weather controls and high-dimensional fixed effects.

Next, we use alternative measures of high-temperature exposure, using equation (2). Results in Table 4 indicate that our baseline findings on cooperation remain robust for these alternative measures. For example, column (1) indicates that increasing cooling degree days by one day raises the expected count of cooperation by 0.32%, and the effect is statistically significant at 1%. The magnitude of the effects estimated in this specification is quantitatively comparable to that estimated in the baseline specification. Moreover, when we use the number of consecutive hot days (T>32°C) in the last 30 days as a measure of high-temperature exposure, the results, reported in columns (5) and (6), are qualitatively consistent.

Next, we examine the effects on different types of cooperation. As reported in Table 5, we find that extreme high temperatures lead to more cooperation of all three types: economy, law, and diplomacy. For example, increasing the number of days in the temperature bin of T>32°C by one day relative to the reference bin leads to an increase of economic and technological cooperation events by 8.51% on average.

5.2 Mechanisms and Heterogeneity Analysis

In this section, we explore the possible mechanisms by which the effects of extreme high temperatures are at play. We first use interaction term variables in regressions to figure out in what situations the

effects of extreme high temperatures are more salient. We find in Table 6 that the effects on cooperation are more salient if the productivity is lower. The results are consistent with the reasoning of opportunity costs: when the return of routine jobs is lower, extreme high temperatures will induce the choice of outside options, since rational decision-makers compare the benefits of different alternatives and choose the best one. This is especially the case for regions with a low productivity that is associated with a smaller opportunity cost. Therefore, the results are supported by Hypothesis 2 and Prediction B2.

We then provide more analysis of the heterogeneity. Again, using interaction term regressions, we find in Table 7 that the positive effects of extreme high temperatures are more salient if labor productivity (not the same as TFP) is lower and if labor is more intensively used in industrial production. Again, these results are consistent with the conceptual framework and the theoretical model in Appendix B.

Next, we examine the spatial spillover effects and the temporal cumulative effects of temperatures. Results in Tables 8 and 9 suggest that extreme high temperatures have spatial spillover and temporal cumulative effects: extreme high temperatures in neighboring cities also exert a significant impact on social dynamics, and temperatures in the past 3-12 months have similar effects. Therefore, inter-regional coordination and continued efforts are made to combat the negative effects of extreme high temperatures and global warming. Moreover, since cooperation may be facilitated before the actual occurrence date, the significance of the cumulative effects also indicates that extreme high temperatures indeed cause more cooperation (in the future). The results are further consistent with the results on lagged effects in Table 10. The results of cumulative effects and lagged effects both imply that past hot days increase future cooperation.

We examine the regional heterogeneity of the effects of extreme high temperatures. According to the results in Table C1, East and Southwest China are the most positively affected by extreme high temperatures. Thus, the impacts of extreme high temperatures exhibit a certain degree of regional heterogeneity. We also examine whether our results are driven by certain seasons. To meet this end, we exclude each of the four seasons, spring, summer, fall, and winter from the sample and rerun the baseline specification. The results in Table C2 exhibit significant heterogeneity. Our estimated main effects in the baseline specification are a weighted average of the effects in different regions and seasons.

5.3 Robustness Checks

In this section, we explore several sets of robustness checks. First, we exploit OLS estimation and use $\log(Y)$ and $arcsinh(Y)$ as the dependent variable. Recent research has shown that doing so may lead to some bias in estimating the true treatment effect (Chen and Roth, 2023), but it is reassuring that we show here that, in Table A3, the results are still qualitatively robust using log transformation of the dependent variables.

Second, we use different ways of clustering standard errors and show that the statistical significance does not change significantly. We report the results in Table A4. For example, in column (1) we cluster the standard error at the city level, and the results consistently show extreme high temperature increases social dynamics.

Third, since it is reasonable that when the cooperation was under negotiation, only a range of dates of final occurrence may be deterministically set, the date that the cooperation occurred may be subject to fuzziness. However, since we use monthly data, it is unlikely that the cooperation happens in a different month than the previously planned date, except for the first and the last days of each month. Therefore, we exclude the first and the last one to three days of each month from the sample and rerun the baseline specification. The results in Table A5 are still similar to the baseline results. Moreover, when we use weekly and daily data to obtain the results respectively in Table A6 and A7, the results are less significant. Thus, due to the fuzziness of cooperation dates, the results are more salient at a more aggregate level. Moreover, the planning stage of the cooperation before occurrence may also be affected by temperatures. Such an argument is supported by Table A8, where the data is aggregated at year and semi-year levels, in which the planning date of the public events and the occurrence date of the public events are more likely to fall into the same interval.

Fourth, we examine whether our results are still robust when we control for air pollution. To meet this end, we add the concentration of PM2.5 and PM10 as the control variables and report the results in Table C3. It is reassuring that the results are still qualitatively similar to the baseline results in Table 1. Thus, our main results are not driven by air pollution.[16]

Fifth, we use the maximum and minimum daily temperatures for robustness checks. Results in Table C4 show that the maximum temperatures do not exert a significant impact, whereas the minimum temperatures do. A high minimum temperature implies an even higher maximum temperature of the same time period, and, thus, may have more salient effects on social dynamics.

Finally, we show the effects of other climate variables in Table C5. All variables, including mean temperature, precipitation, wind speed, and sunshine duration, do not have discernible effects on cooperation. Thus, temperatures have non-linear effects on social dynamics, so that extreme high temperatures are the only salient climate factor that shapes social dynamics, and, this raises concerns about human responses to climate change and global warming.

5.4 Effects on Protests

We also find that extreme high temperatures affect protests. However, according to results reported in Table 11, in our baseline specification, the effects are not statistically significant; they may be significant in other specifications. For example, in column (1), the coefficient is 0.111, and it is not even statistically significant at the 10% level. When we cluster the standard error at the provincial level, the statistical significance rises to the 1% level. Thus, the effects on protests, while interesting and important in their own right, are not the main focus of this paper.

[16]This should be a concern since in another paper of ours (Gong et al., 2024), we argue that (information about) air pollution affects both cooperation and protests.

5.5 Reduced-form Economic Implications of Social Dynamics

In this section, we explore the implications of social dynamics on economic outcomes, using reduced-form estimates. We revisit this issue using a macroeconomic quantitative model in Section 6 below. In Table 12, we find that the number of cooperation is strongly and positively associated with economic output. Thus, although global warming may harm productivity and growth in the long run, the human race and society can adjust and adapt by engaging in more social cooperation that creates more economic opportunities that offset the negative impacts.

We next conduct a back-of-the-envelope calculation of the effects of human adaptation through changing social dynamics. Given the estimates in Table 12, an extra day with extreme high temperature reduces the economic output by 0.47%. Thus, by combining the estimates in Tables 1 and 12, we get that human adaptation via changing social dynamics offsets 34.6% of the negative impacts of extreme high temperatures on the economy.[17] The magnitude of the effects is similar to those given by the quantitative model below.

A caveat in interpreting our results is that in this back-of-the-envelope calculation, we only focus on the effects of human adaptation through the channel of reshaping social dynamics, or increasing social cooperation. It is entirely possible that the economy and society are using other means for adaptation. For example, in response to climate change and global warming, firm behaviors (Shi and Zhang, 2023) and the way of human capital investment (Zhang et al., 2024) may change. We further support the analysis using reduced-form estimates with a quantitative macroeconomic model presented below.

6 Macroeconomic Analyses

In this section, we conduct a set of macroeconomic analyses that complement the reduced-form empirical analyses. The goal of these analyses is to deliver a quantitative result on the impacts of global warming on the economy and the effects of adaptation by social dynamics. We first lay out a novel endogenous growth model that features climate change and adaptation through social dynamics. Social dynamics are also depicted using the same framework as in Appendix B. Thus, this endogenous growth model is the full model that includes the strategic interaction model of collective actions in Appendix B. We next calibrate and estimate the model, and then conduct counterfactual experiments.

The models in this section and in Appendix B play different roles. The model in this section builds a framework for quantitative analysis, whereas the model in Appendix B rationalizes theoretical predictions in the conceptual framework. Again, the model in this section nests that in Appendix B, with some proofs shared in both models.

[17] The formula for computation is: $\frac{8.51 \times 0.0191}{0.47} \times 100\% = 34.6\%$. We make conservative arguments on the causal interpretation of the results in Table 12 columns (2) through (4). They only serve the purpose of conducting a back-of-the-envelope calculation.

6.1 An Endogenous Growth Model

Time t is continuous. There are N representative households (indexed by i), who are all price-takers and whose preference is $U_t = \int_0^t u(C_i(t))e^{-\rho t}dt$, where ρ is the discount rate. To fix the idea, $u(C)$ is a simple CRRA function that preserves homotheticity, $u(C) = \frac{C^{1-\theta}-1}{1-\theta}$.

Cooperation fosters the accumulation of social capital X_t, which plays a role in production. In what follows, we will omit time and household subscripts when it does not cause confusion. Specifically, the production function of the representative firm is $Y = F(K, XL) = AK^{\alpha}(XL)^{1-\alpha}$. $A = A(T)$ is the total factor productivity, which is a function of temperatures, denoted as a capital letter T (time is indexed by a small letter t). Social capital X augments labor productivity. To be specific, $X = g(x)K$, where x is the total contribution of collective action, or social cooperation, and is formulated below, and in a similar way as Appendix B. Social capital is a linear function of physical capital, implying that its contribution to growth is larger when the economy is more developed and equipped with physical capital. These features make the model a standard AK model, since

$$Y = F(K, XL) = AK^{\alpha}(XL)^{1-\alpha} = (g(x)^{1-\alpha}L^{1-\alpha})K, \tag{4}$$

and, thus, the output is a linear function of capital. In the analysis below, we can normalize labor L to one. In the balanced growth path, the growth rate is given by a constant. Consumption and capital both grow at the same constant rate.

Same as the theoretical model in Appendix B, each household i exerts effort a_i to participate in the collective action of social cooperation, in which his contribution x_i is a function of the effort of all agents:

$$x_i = a_i + b(T)\sum_{j\in i} a_j, \tag{5}$$

where T is the temperature, and $b(T) > 0$ is the matching rate of agents and is a strictly increasing function of the temperature. $b(T)$ captures the nature of collective actions since a household's contribution is larger when other households exert more effort. It also captures the difficulty of coordination, which is affected by temperatures, since temperatures serve as a public signal for coordination. In the case of cooperation, extreme high temperatures induce all households to exert effort collectively to combat the damage. The cost of effort is each household's leisure, which is priced at the wage rate w.

$x = \sum_i x_i$ is the total contribution of collective action. Thus, $X = g(x)K = g(\sum_i x_i)K$. For simplicity and to fix the idea, we assume that the $g(\cdot)$ function is linear, and, thus, $X = \phi\sum_i x_i \times K$, where ϕ is a scaling factor.[18] Therefore,

$$Y = F(K, XL) = AK^{\alpha}(XL)^{1-\alpha} = ((\phi\sum_i x_i)^{1-\alpha}L^{1-\alpha})K. \tag{6}$$

At each t, all households play a static game of collective action, which yields the equilibrium level

[18] In robustness checks that are available upon request, the main quantitative results are also similar when we use higher-order polynomials up to fourth order.

of x and X, denoted as x^* and X^*. Thus, each household faces an intratemporal maximization problem to maximize per-period net income:

$$a_i^* = \arg\max_{a_i} r(g(x)K)k + w(g(x)K) - w(g(x)K)a_i, \tag{7}$$

where capital and labor rental rates are both a function of social capital, and, thus, collective action. It is easy to verify that equation (7) is strictly increasing and strictly concave in a_i, given the expression of r and w. Note that all households are price-takers and face the same r and w. We can derive the first-order condition (similar to equation (B5) in Appendix B) and obtain the Nash equilibrium.[19] Then, we can have an equilibrium level of social capital X^* (and x^*).

Each household faces the following budget constraint:

$$\dot{k}(t) = r(t)k(t) + w(t) - c(t) - \delta k(t), \tag{8}$$

where r and w are given by

$$r = \alpha A(T)(\phi x^*(T))^{1-\alpha} L^{1-\alpha}, \tag{9}$$

and,

$$w = (1-\alpha)A(T)(\phi x^*(T))^{1-\alpha} K L^{1-\alpha}, \tag{10}$$

Thus, households take w and r as given, but the equilibrium w and r are shaped by all households' decisions in equilibrium. We focus on a Nash equilibrium for the intratemporal static game.

The rest of the model follows a standard framework of endogenous growth. Households make dynamic optimization decisions regarding capital accumulation. The model features endogenous growth that resembles a standard AK model, in which the Euler equation reads as follows

$$\frac{\dot{C}}{C} = \frac{\dot{K}}{K} = g = \frac{M(T) - \delta - \rho}{\theta}, \tag{11}$$

where $\frac{\dot{C}}{C}$ ($\frac{\dot{K}}{K}$) is the growth rate of consumption (capital), $M(T) = \alpha A(T)(\phi x^*(T))^{1-\alpha} L^{1-\alpha}$ is a constant that is a function of temperatures T. In practice, we can normalize the measure of labor to one, and, thus, $M(T) = \alpha A(T)(\phi x^*(T))^{1-\alpha}$. $M(T)$ is shaped by (1) direct productivity effects, or the effects of T on $A(T)$, and (2) responses of adaptation by social dynamics, or the effects of T on $x^*(T)$, which is also a function of T. In the quantitative analysis, we decompose the effects of temperatures on growth into these two channels. Due to the multiplicative nature of equation (11), the channel of productivity can be written as $\frac{d \log A(T)}{dT}$, and the channel of adaptation can be written as $(1-\alpha) \times \frac{d \log x^*(T)}{dT}$. Therefore, equation (11) illustrates how human society adapts to climate change by reshaping social dynamics. We have the following proposition to illustrate such an adaptation.

[19] The system of equations does not produce analytical solutions. Therefore, we only obtain numerical solutions in the quantitative analysis. Meanwhile, the theoretical results do not rely on the analytical form of the solutions.

Proposition 1. *Due to the response of social dynamics, or cooperation by a higher $x^*(T)$, the negative impacts of global warming on the economy are smaller.*

The proof is isomorphic to that of Prediction B1, since households also face a concave objective function (7). Thus, we can obtain the result of the monotonicity of the relationship between temperatures and social cooperation. □

6.2 Quantitative Analysis

6.2.1 Calibration

First, we parameterize $A(T)$, $b(T)$, and $g(x)$. Without loss of generality, we set $A(T) = \sum_\tau a_\tau D_\tau$[20] as a linear function of temperature bins D_τ, and is estimated using reduced-form regression. We also set $b(T) = \sum_\tau a_\tau D_\tau$ as a linear function of temperature bins, and is estimated using matching moments of social cooperation of the data and the model. $g(x)$ is manually set as a linear function $g(x) = \phi \times x$.

We calibrate the discount factor and the intertemporal elasticity of substitution using the results of the existing literature. Following Acemoglu et al. (2018), we set the discount rate equal to $\rho = 2\%$, which corresponds to an annual discount factor of 97% (Song et al., 2011). Also, following Acemoglu et al. (2018), we set the inverse of the intertemporal elasticity of substitution $\theta = 2$. α is set as 0.42 to match the labor income share in 2019.

We estimate $\{a_\tau\}$ using a production function estimation approach and the Annual Survey of Industrial Firm (ASIF) data. We first obtain firm-level total factor productivity using the OP-ACF-correction approach (Ackerberg et al., 2015), and then estimate the productivity counterpart of equation (1). We calibrate $\{\phi, b_\tau\}$ by matching the model moments with the data moments of economic outputs and social capital (measured by the counts of cooperation events). We calculate the standard errors by Bootstrap. Table C6 shows that the model moments can match the data moments well.[21] b_τ can then be identified using temperature variations across different localities. The estimate of ϕ is 0.375, with a standard error being 0.0446. The rest of the parameter estimates are reported in Table A9. High temperatures significantly reduce productivity and increase the matching rate of cooperation. The former result is consistent with Zhang et al. (2018) and Shi and Zhang (2023), and the latter result is consistent with the baseline results in Table 1.

6.2.2 Counterfactual Analysis

In this section, we calculate the contributions of global warming to economic growth, and decompose the contributions into two channels: (1) the direct productivity effect, and (2) adaptation via reshaping social dynamics. To meet this end, we fix the equilibrium outcomes associated with one channel, and then evaluate the effects of the other channel. Moreover, due to the multiplicative nature of equation

[20] Note that this specification is consistent with the baseline econometric specification.

[21] Specifically, we match the moments of cooperation of the entire country and each province.

(11), the channel of productivity can be written as $\frac{d \log A(T)}{dT}$, and the channel of adaptation can be written as $(1-\alpha) \times \frac{d \log x^*(T)}{dT}$.

We first analyze the potential impacts of projected (2070-2099) global warming. We obtain the temperature projection at the city level, and calculate the impacts of such a projection on economic growth. In particular, we decompose the total effects into (1) the direct productivity effect, and (2) the adaptation by social dynamics. We plot the effects at the city level. Figure 3 presents the results. On average, the projected global warming reduces the growth rate by 0.19%, but adaptation by social dynamics/cooperation offsets about one-third of the negative impacts. Therefore, the quantitative model yields similar results compared to the reduced-form estimates. The effects are more salient for Huabei and Huadong regions, since there is a more significant increase in temperatures in these areas.

We next analyze the impacts of policy responses. We hypothetically subsidize labor (by increasing w directly), capital (by increasing r directly), and cooperation (by increasing $b(T)$ directly), and study their impacts on the equilibrium growth rate. We report these counterfactual experiments in Table 13. Subsidizing labor, capital, and collective action by 5% leads to an increase in growth rate by 0.275%, 1.280%, and 1.679%, respectively. This pattern holds for all degrees of subsidy. Increasing subsidies also increases the equilibrium growth rate, but at a declining margin. Thus, directly subsidizing cooperation is the most effective way to foster adaptation via social dynamics. Subsidizing labor is the least effective since it raises the opportunity cost of cooperation. Such results provide guidance for a cost-benefit analysis for policymakers.

7 Conclusion

Using a novel city-monthly panel data set of public events in China, we are among the first in the literature to document that extreme high temperatures significantly reshape social dynamics. Using Poisson regressions with high-dimensional fixed effects, we find that extreme high temperatures lead to an increase in social cooperation. Evidence supports the explanation that extreme high temperatures boost the relative returns of cooperation given lowered productivity, which is all consistent with a conceptual framework and a theoretical model of collective actions. Our main results survive in an array of robustness checks, including different linear and non-linear estimation strategies, different measures of dependent variables, the inclusion of various sets of control variables and high-dimensional fixed effects, and different ways of clustering standard errors.

In addition, we also find that extreme high temperatures have regional spillover and temporal accumulative effects, suggesting the role of regional coordination and continued attention to the harm of global warming. Policymakers in different localities can utilize this finding to align inter-regional interests and foster regional cooperation to adapt to climate change together.

Finally, we build an endogenous growth model with climate change and adaptation via collective actions, or social dynamics. We calibrate the model and conduct counterfactual experiments. We find that adaptation by social dynamics offsets about one-third of the negative impacts of global warming on the economy. The magnitude is similar to the result of the back-of-the-envelope calculation using

reduced-form estimates. Moreover, we find that directly subsidizing social cooperation is much more effective than subsidizing labor and capital rental in combating the negative impacts of global warming, since social cooperation is shown to be the main adaptation mechanism at play.

The main contribution of our paper is to document the response of social dynamics to extreme high temperatures, or more broadly, the trending climate change. Our results suggest that the economy and society may resort to more economic cooperation to combat the negative impacts of global warming. Future research can further explore the social impacts of temperatures, climate, and other environmental factors. Finally, this paper focuses on China, but our analyses can be readily extended to other developing countries.

References

[1] G. Abel, L. Plumridge, and P. Graham. Peers, networks or relationships: strategies for understanding social dynamics as determinants of smoking behaviour. *Drugs: education, prevention and policy*, 9(4): 325–338, 2002.

[2] D. Acemoglu, U. Akcigit, H. Alp, N. Bloom, and W. Kerr. Innovation, reallocation, and growth. *American Economic Review*, 108(11):3450–91, 2018.

[3] D. A. Ackerberg, K. Caves, and G. Frazer. Identification properties of recent production function estimators. *Econometrica*, 83(6):2411–2451, 2015.

[4] S. Agarwal, Y. Qin, L. Shi, G. Wei, and H. Zhu. Impact of temperature on morbidity: New evidence from china. *Available at SSRN 3807776*, 2021.

[5] M. Auffhammer. Quantifying economic damages from climate change. *Journal of Economic Perspectives*, 32(4):33–52, 2018.

[6] J. Bai and P. Perron. Estimating and testing linear models with multiple structural changes. *Econometrica*, pages 47–78, 1998.

[7] J. Bai and P. Perron. Computation and analysis of multiple structural change models. *Journal of applied econometrics*, 18(1):1–22, 2003.

[8] R. Banerjee and R. Maharaj. Heat, infant mortality, and adaptation: Evidence from india. *Journal of Development Economics*, 143:102378, 2020.

[9] A. Barreca, K. Clay, O. Deschenes, M. Greenstone, and J. S. Shapiro. Adapting to climate change: The remarkable decline in the us temperature-mortality relationship over the twentieth century. *Journal of Political Economy*, 124(1):105–159, 2016.

[10] P. Barrett, M. Appendino, K. Nguyen, and J. de Leon Miranda. Measuring social unrest using media reports. *Journal of Development Economics*, 158:102924, 2022.

[11] M. Beraja, A. Kao, D. Y. Yang, and N. Yuchtman. Ai-tocracy. *The Quarterly Journal of Economics*, 138(3):1349–1402, 2023.

[12] L. Bursztyn, D. Cantoni, D. Y. Yang, N. Yuchtman, and Y. J. Zhang. Persistent political engagement: Social interactions and the dynamics of protest movements. *American Economic Review: Insights*, 3(2): 233–250, 2021.

[13] D. Cantoni, D. Y. Yang, N. Yuchtman, and Y. J. Zhang. Protests as strategic games: experimental evidence from hong kong's antiauthoritarian movement. *The Quarterly Journal of Economics*, 134(2): 1021–1077, 2019.

[14] D. Cantoni, A. Kao, D. Y. Yang, and N. Yuchtman. Protests. Technical report, National Bureau of Economic Research, 2023.

[15] J. Chen and J. Roth. Logs with zeros? some problems and solutions. *The Quarterly Journal of Economics*, page qjad054, 2023.

[16] X. Cui and Q. Tang. Extreme heat and rural household adaptation: Evidence from northeast china. *Journal of Development Economics*, 167:103243, 2024.

[17] M. Dell, B. F. Jones, and B. A. Olken. Temperature and income: reconciling new cross-sectional and panel estimates. *American Economic Review*, 99(2):198–204, 2009.

[18] M. Dell, B. F. Jones, and B. A. Olken. Temperature shocks and economic growth: Evidence from the last half century. *American Economic Journal: Macroeconomics*, 4(3):66–95, 2012.

[19] M. Dell, B. F. Jones, and B. A. Olken. What do we learn from the weather? the new climate-economy literature. *Journal of Economic literature*, 52(3):740–798, 2014.

[20] O. Deschênes and M. Greenstone. The economic impacts of climate change: evidence from agricultural output and random fluctuations in weather. *American economic review*, 97(1):354–385, 2007.

[21] O. Deschênes and M. Greenstone. Climate change, mortality, and adaptation: Evidence from annual fluctuations in weather in the us. *American Economic Journal: Applied Economics*, 3(4):152–85, 2011.

[22] J. Gong, X. Shi, C. Wang, and X. Zhang. The dilemma of pollution information disclosure: Evidence from a new data set. *Available at SSRN*, 2024.

[23] J. M. Guttman. Understanding collective action: matching behavior. *The American Economic Review*, 68(2):251–255, 1978.

[24] Y. Hua, Y. Qiu, and X. Tan. The effects of temperature on mental health: evidence from china. *Journal of Population Economics*, 36(3):1293–1332, 2023.

[25] Y. Huang and Y. Li. Labor activism over searing heat. *Journal of Environmental Economics and Management*, 122:102888, 2023.

[26] J. Levinsohn and A. Petrin. Estimating production functions using inputs to control for unobservables. *The review of economic studies*, 70(2):317–341, 2003.

[27] J. Li and G. Meng. Pollution exposure and social conflicts: Evidence from china's daily data. *Journal of Environmental Economics and Management*, 121:102870, 2023.

[28] M. LoPalo. Temperature, worker productivity, and adaptation: evidence from survey data production. *American Economic Journal: Applied Economics*, 15(1):192–229, 2023.

[29] A. Marchand, T. Hennig-Thurau, and J. Flemming. Social media resources and capabilities as strategic determinants of social media performance. *International Journal of Research in Marketing*, 38(3):549–571, 2021.

[30] E. W. Montroll. Social dynamics and the quantifying of social forces. *Proceedings of the National Academy of Sciences*, 75(10):4633–4637, 1978.

[31] J. T. Mullins and C. White. Temperature and mental health: Evidence from the spectrum of mental health outcomes. *Journal of health economics*, 68:102240, 2019.

[32] N. Obradovich, R. Migliorini, M. P. Paulus, and I. Rahwan. Empirical evidence of mental health risks posed by climate change. *Proceedings of the National Academy of Sciences*, 115(43):10953–10958, 2018.

[33] B. A. Olken. Do television and radio destroy social capital? evidence from indonesian villages. *American Economic Journal: Applied Economics*, 1(4):1–33, 2009.

[34] G. S. Olley and A. Pakes. The dynamics of productivity in the telecommunications equipment. *Econometrica*, 64(6):1263–1297, 1996.

[35] F. Polletta and J. M. Jasper. Collective identity and social movements. *Annual review of Sociology*, 27 (1):283–305, 2001.

[36] M. Shah and B. M. Steinberg. Drought of opportunities: Contemporaneous and long-term impacts of rainfall shocks on human capital. *Journal of Political Economy*, 125(2):527–561, 2017.

[37] X. Shi and X. Zhang. Reevaluating the productivity effects of extreme high temperatures from the perspective of firm dynamics: The case of chinese manufacturing. *Available at SSRN 4380448*, 2023.

[38] R. J. Shiller, S. Fischer, and B. M. Friedman. Stock prices and social dynamics. *Brookings papers on economic activity*, 1984(2):457–510, 1984.

[39] Z. Song, K. Storesletten, and F. Zilibotti. Growing like china. *American economic review*, 101(1): 196–233, 2011.

[40] S. J. Wallace, C. Zepeda-Millán, and M. Jones-Correa. Spatial and temporal proximity: Examining the effects of protests on political attitudes. *American Journal of Political Science*, 58(2):433–448, 2014.

[41] D. Wang, P. Zhang, S. Chen, and N. Zhang. Adaptation to temperature extremes in chinese agriculture, 1981 to 2010. *Journal of Development Economics*, 166:103196, 2024.

[42] X. Yu, X. Lei, and M. Wang. Temperature effects on mortality and household adaptation: Evidence from china. *Journal of Environmental Economics and Management*, 96:195–212, 2019.

[43] P. Zhang, O. Deschenes, K. Meng, and J. Zhang. Temperature effects on productivity and factor reallocation: Evidence from a half million chinese manufacturing plants. *Journal of Environmental Economics and Management*, 88:1–17, 2018.

[44] X. Zhang, X. Chen, and X. Zhang. Temperature and low-stakes cognitive performance. *Journal of the Association of Environmental and Resource Economists*, 11(1):75–96, 2024.

[45] J. G. Zivin and M. E. Kahn. Industrial productivity in a hotter world: the aggregate implications of heterogeneous firm investment in air conditioning. Technical report, National Bureau of Economic Research, 2016.

[46] J. G. Zivin, Y. Song, Q. Tang, and P. Zhang. Temperature and high-stakes cognitive performance: Evidence from the national college entrance examination in china. *Journal of Environmental Economics and Management*, 104:102365, 2020.

Figure 1: Data descriptive analysis

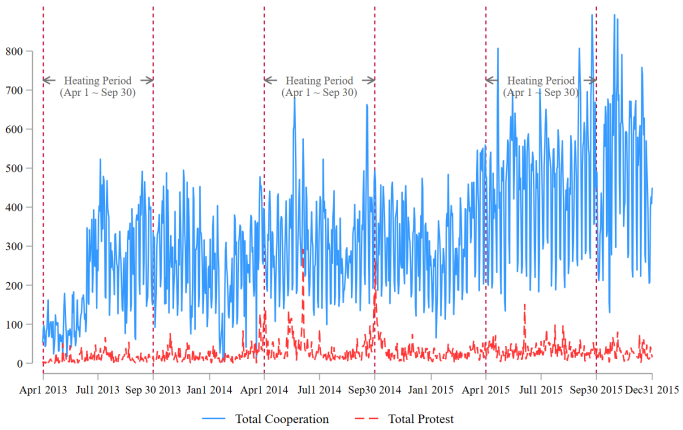

(a)

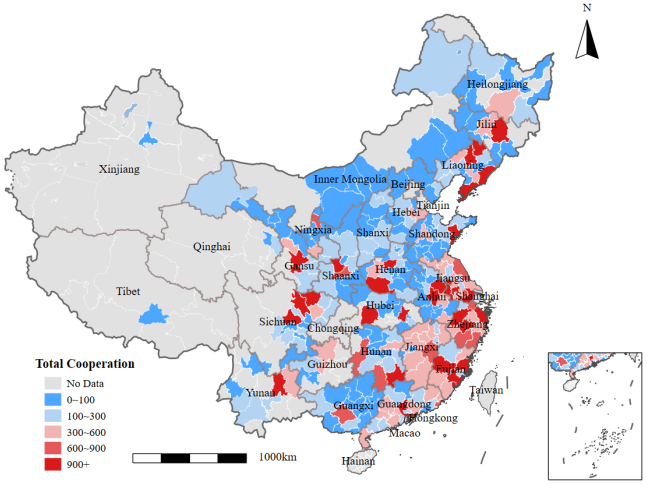

(b)

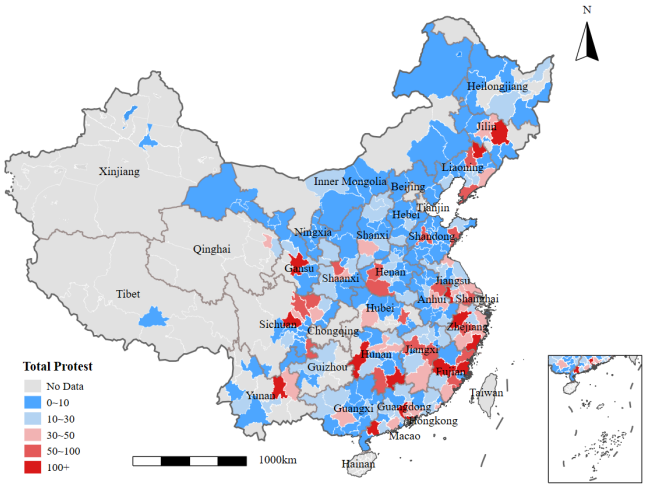

(c)

Notes: Figure 1 (a) presents the time series of public events, Figures 1 (b) and (c) shows the spatial distribution of public events. The sample coverage is 2013-2015.

Figure 2: Regression coefficients plot

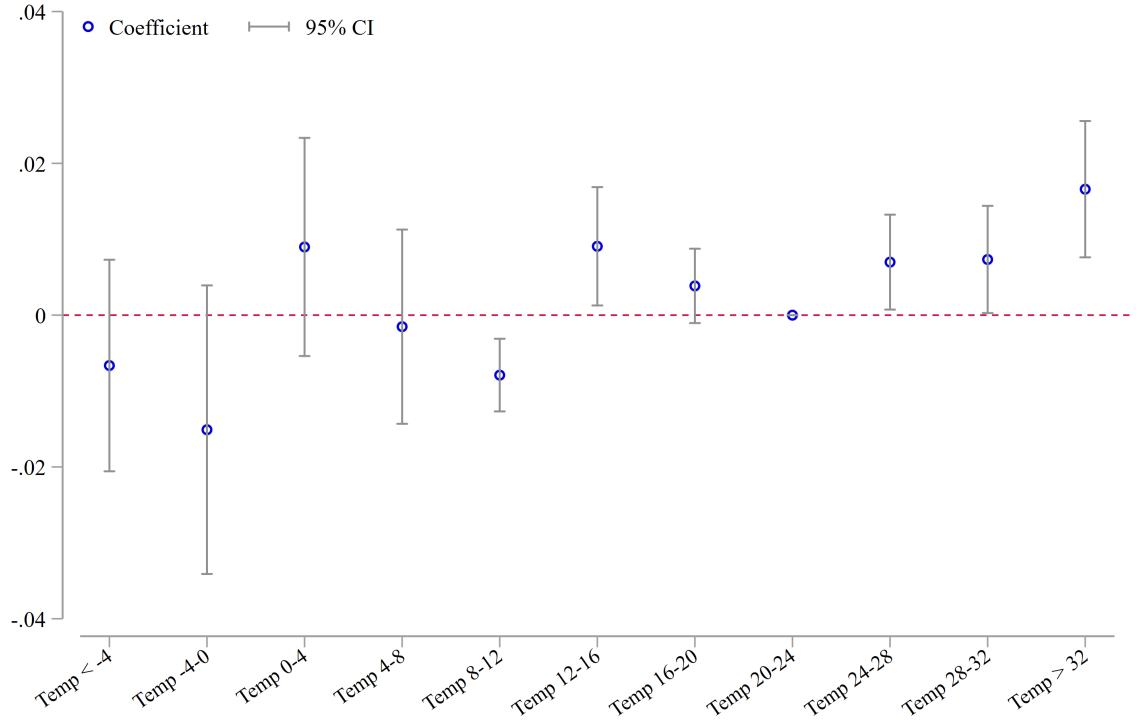

Notes: Figure 2 plots the regression coefficients in Table 1, column (2). The sample coverage is 2013-2015. The temperature bins are in Celsius.

Figure 3: Effects of projected global warming

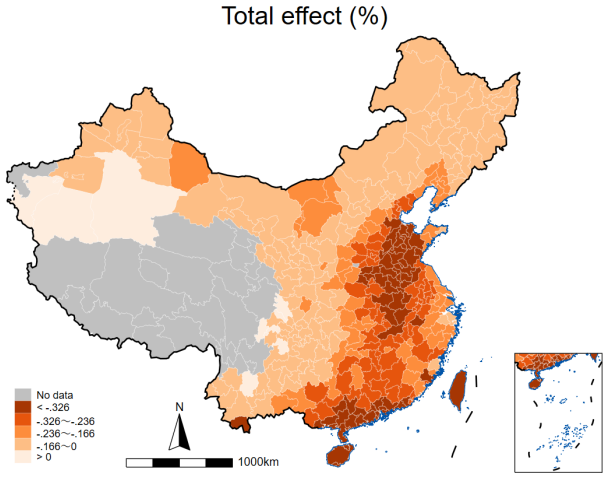

(a)

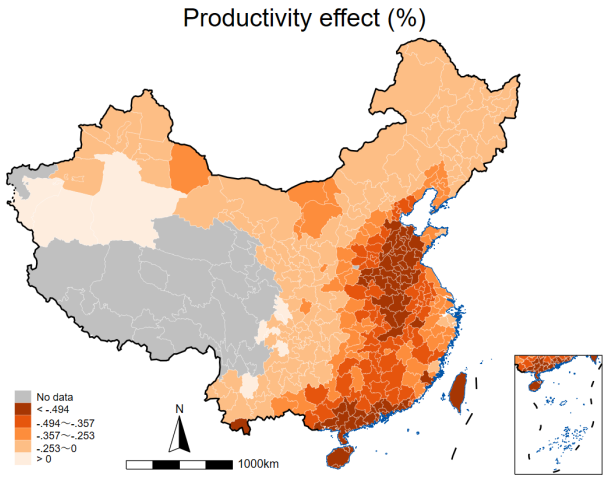

(b)

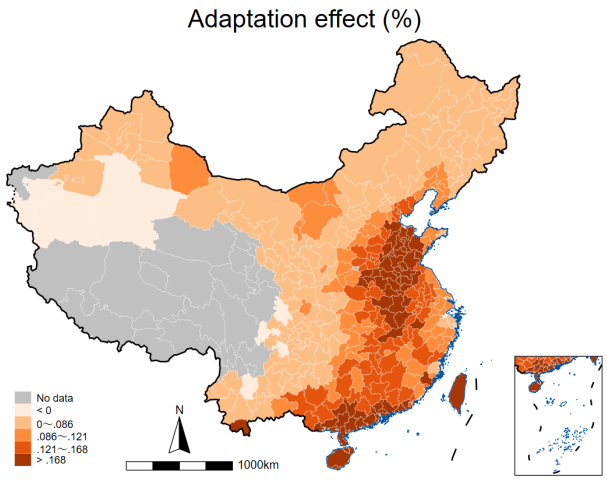

(c)

Notes: Figure 3 (a) presents the total effects of projected global warming on economic growth, Figures 3 (b) and (c) shows the channel of productivity effects and adaptation through social dynamics/cooperation.

Table 1: Baseline results

	(1)	(2)
	Cooperation (total)	
	PPML	
Temp>32	0.0507***	0.0176***
	(0.0148)	(0.00490)
Temp 28-32	0.0141	0.00875***
	(0.0144)	(0.00301)
Temp 24-28	0.0105	0.00752**
	(0.0112)	(0.00300)
Temp 16-20	0.0179**	0.00376
	(0.00881)	(0.00247)
Temp 12-16	0.0484***	0.00869**
	(0.0173)	(0.00376)
Temp 8-12	0.0659**	-0.00859***
	(0.0276)	(0.00265)
Temp 4-8	0.0628**	-0.00207
	(0.0316)	(0.00679)
Temp 0-4	0.0475*	0.00850
	(0.0254)	(0.00682)
Temp -4-0	0.0435**	-0.0152
	(0.0195)	(0.0101)
Temp<-4	0.00519	-0.00806
	(0.0214)	(0.00715)
Observations	9,804	9,816
Weather Controls	Yes	Yes
City-Month FE	Yes	No
City-Year FE	Yes	Yes
Year-Month FE	No	Yes
Period	Jan 2013-Dec 2015	
Level	City-Year-Month	

Notes: The sample covers about 9,800 city-year-month observations (273 cities and 36 months) from January 2013 to December 2015. We employ Poisson Pseudo Maximum Likelihood (PPML) regressions for all columns. Total cooperation is measured by the number of cooperation events. Temperature bins are measured by the monthly number of days with daily mean temperature in the corresponding temperature range. Temperature bin 20-24°C is chosen as the reference bin. Weather controls include precipitation, wind speed, and relative humidity. *** p<0.01, ** p<0.05, * p<0.1. The standard errors are two-way clustered at the city and year levels.

Table 2: Controlling for high orders of weather controls

	(1)	(2)	(3)
	Cooperation (total)		
	PPML		
Temp>32	0.0160***	0.0184***	0.0189**
	(0.00548)	(0.00499)	(0.00866)
Temp 28-32	0.00619	0.00568	0.00517
	(0.00400)	(0.00421)	(0.00530)
Temp 24-28	0.00634**	0.00604	0.00591
	(0.00321)	(0.00480)	(0.00396)
Temp 16-20	0.00395	0.00409	0.00417
	(0.00293)	(0.00306)	(0.00640)
Temp 12-16	0.00981***	0.0104	0.0105**
	(0.00372)	(0.00640)	(0.00463)
Temp 8-12	-0.00667***	-0.00589*	-0.00540
	(0.00257)	(0.00307)	(0.00930)
Temp 4-8	-0.00121	-0.000255	-0.000458
	(0.00624)	(0.00732)	(0.00940)
Temp 0-4	0.00993	0.0105	0.0103
	(0.00732)	(0.00924)	(0.0103)
Temp -4-0	-0.0137	-0.0122	-0.0128
	(0.00989)	(0.0139)	(0.0132)
Temp<-4	-0.00559	-0.00485	-0.00515
	(0.00697)	(0.00855)	(0.00798)
Observations	9,816	9,816	9,816
Weather controls	Yes	Yes	Yes
Quadratic weather controls	Yes	Yes	Yes
Cubic weather controls	No	Yes	Yes
Quartic weather controls	No	No	Yes
City-Year FE	Yes	Yes	Yes
Year-Month FE	Yes	Yes	Yes
Period	Jan 2013-Dec 2015		
Level	City-Year-Month		

Notes: The sample covers about 9,800 city-year-month observations (273 cities and 36 months) from January 2013 to December 2015. We employ Poisson Pseudo Maximum Likelihood (PPML) regressions for all columns. Total cooperation is measured by the number of cooperation events. Temperature bins are measured by the monthly number of days with daily mean temperature in the corresponding temperature range. Temperature bin 20-24°C is chosen as the reference bin. Weather controls include precipitation, wind speed, and relative humidity. Compared to the baseline specification, Columns (1)-(3) respectively add quadratic, quadratic, and cubic, and quadratic, cubic, and quartic weather controls. *** p<0.01, ** p<0.05, * p<0.1. The standard errors are two-way clustered at the city and year levels.

Table 3: Results of controlling for alternative fixed effects

	(1)	(2)	(3)	(4)	(5)
	Cooperation (total)				
	PPML				
Temp>32	0.0421**	0.0370***	0.0176***	0.0421**	0.0370***
	(0.0203)	(0.00741)	(0.00490)	(0.0203)	(0.00741)
Temp 28-32	0.0108	0.0104*	0.00875***	0.0108	0.0104*
	(0.0196)	(0.00573)	(0.00301)	(0.0196)	(0.00573)
Observations	9,792	9,816	9,816	9,792	9,816
Weather Controls	Yes	Yes	Yes	Yes	Yes
City-Year FE	Yes	Yes	Yes	Yes	Yes
Year-Month FE	No	No	Yes	No	No
Province-Year-Month FE	Yes	No	No	Yes	No
Province-Year-Season FE	No	Yes	No	No	Yes
City-Year-Month Linear Trend	No	No	Yes	Yes	Yes
Period	Jan 2013-Dec 2015				
Level	City-Year-Month				
Mean of Y	12.44	12.41	12.41	12.44	12.41
SD of Y	39.33	39.29	39.29	39.33	39.29

Notes: The sample covers about 9,800 city-year-month observations (273 cities and 36 months) from January 2013 to December 2015. We employ Poisson Pseudo Maximum Likelihood (PPML) regressions for all columns. Total cooperation is measured by the number of cooperation events. Temperature bins are measured by the monthly number of days with daily mean temperature in the corresponding temperature range. Temperature bin 20-24°C is chosen as the reference bin. Weather controls include precipitation, wind speed, and relative humidity. *** p<0.01, ** p<0.05, * p<0.1. The standard errors are two-way clustered at the city and year levels.

Table 4: Alternative measures of extreme high temperature exposure

	(1)	(2)	(3)	(4)	(5)	(6)
			Cooperation (total)			
			PPML			
Cooling degree days > 24°C	0.0032*	0.0010***				
	(0.0018)	(0.0004)				
Temp > mean+2SD			0.1340**	0.0941***		
			(0.0592)	(0.0244)		
Consecutive days > 32°C					0.0486***	0.0110**
					(0.0106)	(0.0043)
Observations	9,804	9,816	9,804	9,816	9,804	9,816
Weather Controls	Yes	Yes	Yes	Yes	Yes	Yes
City-Month FE	Yes	No	Yes	No	Yes	No
City-Year FE	Yes	Yes	Yes	Yes	Yes	Yes
Year-Month FE	No	Yes	No	Yes	No	Yes
Period			Jan 2013-Dec 2015			
Level			City-Year-Month			
Mean of Y	12.43	12.41	12.43	12.41	12.43	12.41
SD of Y	39.31	39.29	39.31	39.29	39.31	39.29

Notes: The sample covers about 9,800 city-year-month observations (273 cities and 36 months) from January 2013 to December 2015. We employ Poisson Pseudo Maximum Likelihood (PPML) regressions for all columns. Total cooperation is measured by the number of cooperation events. Cooling degree days>24°C are measured by the average number of degrees by which the daily mean temperature exceeds 24°C, with values below 24°C assigned a value of 0. Temp>mean+2SD are measured by the number of days with daily mean temperature above the historical mean+2SD of daily temperatures during 1980-2010 for each city. Consecutive days>32°C are measured by the number of consecutive days with a daily mean temperature above 32°C. Weather controls include precipitation, wind speed, and relative humidity. *** p<0.01, ** p<0.05, * p<0.1. The standard errors are two-way clustered at the city and year levels.

Table 5: Different types of cooperation

	(1)	(2)	(3)	(4)	(5)	(6)
	Coop. (econ & tech)	Coop. (law)	Coop. (diplomatic)	Coop. (econ & tech)	Coop. (law)	Coop. (diplomatic)
			PPML			
Temp>32	0.0851***	0.409**	0.0315*	0.0261***	0.0160	0.0198**
	(0.0274)	(0.185)	(0.0175)	(0.00756)	(0.0461)	(0.00799)
Temp 28-32	-0.0124	0.0392	0.0112	-0.00819	0.0189	0.0107***
	(0.0173)	(0.0575)	(0.0118)	(0.00625)	(0.0339)	(0.00305)
Temp 24-28	0.00685	0.0679*	0.00584	0.00228	0.0429***	0.00680
	(0.0119)	(0.0403)	(0.0116)	(0.00471)	(0.00755)	(0.00513)
Temp 16-20	0.0452***	-0.0464	0.0130	0.0103	0.00800	0.00259
	(0.0137)	(0.0573)	(0.00963)	(0.00642)	(0.0193)	(0.00423)
Temp 12-16	0.0782***	0.152**	0.0433**	0.00584	0.0595**	0.00878**
	(0.0175)	(0.0663)	(0.0176)	(0.00763)	(0.0243)	(0.00446)
Temp 8-12	0.121***	0.154**	0.0534**	0.00651	0.00240	-0.0111***
	(0.0338)	(0.0628)	(0.0251)	(0.00888)	(0.0226)	(0.00330)
Temp 4-8	0.109***	0.0700	0.0554*	0.00623	0.0304	-0.00283
	(0.0309)	(0.0661)	(0.0291)	(0.0130)	(0.0501)	(0.00779)
Temp 0-4	0.0548*	0.000683	0.0515**	0.00438	-0.0775	0.0144**
	(0.0289)	(0.0635)	(0.0242)	(0.00764)	(0.0600)	(0.00715)
Temp -4-0	0.0545*	0.110***	0.0424**	0.0104	0.0375	-0.0210*
	(0.0284)	(0.0398)	(0.0205)	(0.0150)	(0.124)	(0.0125)
Temp <-4	0.0109	0.364***	0.00558	0.00114	0.0124	-0.00714
	(0.0506)	(0.0562)	(0.0250)	(0.0147)	(0.0359)	(0.00849)
Observations	9,804	9,804	9,804	9,816	9,816	9,816
Weather Controls	Yes	Yes	Yes	Yes	Yes	Yes
City-Month FE	Yes	Yes	Yes	No	No	No
City-Year FE	Yes	Yes	Yes	Yes	Yes	Yes
Year-Month FE	No	No	No	Yes	Yes	Yes
Period			Jan 2013-Dec 2015			
Level			City-Year-Month			
Mean of Y	1.635	0.280	8.881	1.633	0.280	8.870
SD of Y	6.169	2.193	30.56	6.165	2.192	30.55

Notes: The sample covers about 9,800 city-year-month observations (273 cities and 36 months) from January 2013 to December 2015. We employ Poisson Pseudo Maximum Likelihood (PPML) regressions for all columns. Total cooperation is measured by the number of cooperation events. Temperature bins are measured by the monthly number of days with daily mean temperature in the corresponding temperature range. Temperature bin 20-24°C is chosen as the reference bin. Weather controls include precipitation, wind speed, and relative humidity. *** p<0.01, ** p<0.05, * p<0.1. The standard errors are two-way clustered at the city and year levels.

Table 6: Mechanisms: Heterogeneous effects of temperatures

	(1)	(2)	(3)	(4)
	Cooperation (total)			
	PPML			
Temp>32	0.0321***	0.0358***	0.0325**	0.0377*
	(0.00437)	(0.0100)	(0.0133)	(0.0169)
Temp>32*Median TFP (OP)	-0.0317**			
	(0.0144)			
Temp>32*Median TFP (OP, ACF)		-0.0356*		
		(0.0179)		
Temp>32*Median TFP (LP)			-0.0421**	
			(0.0201)	
Temp>32*Median TFP (LP, ACF)				-0.0323*
				(0.0155)
Observations	9,816	9,816	9,816	9,816
Weather Controls	Yes	Yes	Yes	Yes
City-Year FE	Yes	Yes	Yes	Yes
Year-Month FE	Yes	Yes	Yes	Yes
Period		Jan 2013-Dec 2015		
Level		City-Year-Month		
Mean of Y	12.41	12.41	12.41	12.41
SD of Y	39.29	39.29	39.29	39.29

Notes: The sample covers about 9,800 city-year-month observations (273 cities and 36 months) from January 2013 to December 2015. We employ Poisson Pseudo Maximum Likelihood (PPML) regressions for all columns. Total cooperation is measured by the number of cooperation events. Temperature bins are measured by the monthly number of days with daily mean temperature in the corresponding temperature range. Temperature bin 20-24°C is chosen as the reference bin. Weather controls include precipitation, wind speed, and relative humidity. The total factor productivity (TFP) is measured using the median of the period of 1998-2007 with the Annual Survey of Industrial Firms (ASIF) data. *** $p<0.01$, ** $p<0.05$, * $p<0.1$. The standard errors are two-way clustered at the city and year levels.

Table 7: More heterogeneous effects of extreme high temperatures

	(1)	(2)	(3)
	Cooperation (total)		
	PPML		
Temp>32	0.0299***	0.0347***	0.0329**
	(0.00552)	(0.00881)	(0.0113)
Temp>32*Median Labor Productivity	-0.0344**		
	(0.0139)		
Temp>32*Median Labor Intensity		0.0246*	
		(0.0149)	
Temp>32*Median Labor Wage Bill Share			0.0323**
			(0.0151)
Observations	9,816	9,816	9,816
Weather Controls	Yes	Yes	Yes
City-Year FE	Yes	Yes	Yes
Year-Month FE	Yes	Yes	Yes
Period	Jan 2013-Dec 2015		
Level	City-Year-Month		
Mean of Y	12.41	12.41	12.41
SD of Y	39.29	39.29	39.29

Notes: The sample covers about 9,800 city-year-month observations (273 cities and 36 months) from January 2013 to December 2015. We employ Poisson Pseudo Maximum Likelihood (PPML) regressions for all columns. Total cooperation is measured by the number of cooperation events. Temperature bins are measured by the monthly number of days with daily mean temperature in the corresponding temperature range. Temperature bin 20-24°C is chosen as the reference bin. Weather controls include precipitation, wind speed, and relative humidity. The labor productivity, labor intensity, and labor share are measured using the median of the period of 1998-2007 with the Annual Survey of Industrial Firms (ASIF) data. *** p<0.01, ** p<0.05, * p<0.1. The standard errors are two-way clustered at the city and year levels.

Table 8: Spatial spillover effects of extreme high temperatures

	(1)	(2)
	Cooperation (total)	
	PPML	
	Mean of same province	Mean of neighboring cities
Temp>32	0.0677**	0.0668**
	(0.0322)	(0.0331)
Temp 28-32	0.0107	0.0102
	(0.0166)	(0.0161)
Temp 24-28	0.000510	-0.00102
	(0.0136)	(0.0128)
Temp 16-20	0.0139	0.0128
	(0.0134)	(0.0131)
Temp 12-16	0.0644***	0.0643***
	(0.0208)	(0.0203)
Temp 8-12	0.0703**	0.0693**
	(0.0337)	(0.0329)
Temp 4-8	0.0796**	0.0796**
	(0.0388)	(0.0384)
Temp 0-4	0.0483**	0.0469**
	(0.0213)	(0.0200)
Temp -4-0	0.0657*	0.0659*
	(0.0369)	(0.0373)
Temp<-4	0.000842	-0.000567
	(0.0245)	(0.0253)
Observations	9,816	9,816
Weather Controls	Yes	Yes
City-Month FE	Yes	Yes
City-Year FE	Yes	Yes
Year-Month FE	Yes	Yes
Period	Jan 2013-Dec 2015	
Level	City-Year-Month	
Mean of Y	12.41	12.41
SD of Y	39.29	39.29

Notes: The sample covers about 9,800 city-year-month observations (273 cities and 36 months) from January 2013 to December 2015. We employ Poisson Pseudo Maximum Likelihood (PPML) regressions for all columns. Total cooperation is measured by the number of cooperation events. Temperature bins are measured by the monthly number of days with daily mean temperature in the corresponding temperature range. Temperature bin 20-24°C is chosen as the reference bin. Weather controls include precipitation, wind speed, and relative humidity. *** p<0.01, ** p<0.05, * p<0.1. The standard errors are two-way clustered at the city and year levels.

Table 9: Cumulative effects of extreme high temperatures

	(1)	(2)	(3)
	Cooperation (total)		
	PPML		
	3 months	6 months	12 months
Temp>32	0.0426***	0.0733***	0.0305**
	(0.00654)	(0.0200)	(0.0146)
Temp 28-32	0.0201***	0.0229**	0.0149*
	(0.00748)	(0.00940)	(0.00785)
Temp 24-28	0.0164*	0.0262***	0.0121*
	(0.00840)	(0.0100)	(0.00651)
Temp 16-20	0.00598	-0.00560	0.00211
	(0.00738)	(0.00753)	(0.0105)
Temp 12-16	0.0358**	0.0109	0.00159
	(0.0152)	(0.0193)	(0.0145)
Temp 8-12	0.0475**	0.0106	0.00327
	(0.0199)	(0.0177)	(0.0143)
Temp 4-8	0.0444	0.00855	-0.00876
	(0.0278)	(0.0243)	(0.00824)
Temp 0-4	0.0230	0.00718	0.0161
	(0.0184)	(0.0308)	(0.0212)
Temp -4-0	0.0263***	-0.00338	-0.00759
	(0.00999)	(0.0169)	(0.00771)
Temp<-4	-0.0271	-0.0330***	-0.0196***
	(0.0260)	(0.00840)	(0.00739)
Observations	9,816	9,816	9,816
Weather Controls	Yes	Yes	Yes
City-Month FE	Yes	Yes	Yes
City-Year FE	Yes	Yes	Yes
Year-Month FE	Yes	Yes	Yes
Period	2013-2015		
Level	City-Year-Month		
Mean of Y	12.41	12.41	12.41
SD of Y	39.29	39.29	39.29
Mean of X	0.338	0.670	1.385
SD of X	2.053	3.019	4.314

Notes: The sample covers about 9,800 city-year-month observations (273 cities and 36 months) from January 2013 to December 2015. We employ Poisson Pseudo Maximum Likelihood (PPML) regressions for all columns. Total cooperation is measured by the number of cooperation events. Temperature bins are measured by the monthly number of days with daily mean temperature in the corresponding temperature range. Temperature bin 20-24°C is chosen as the reference bin. Weather controls include precipitation, wind speed, and relative humidity. *** p<0.01, ** p<0.05, * p<0.1. The standard errors are two-way clustered at the city and year levels.

Table 10: Lagged effects

	(1)	(2)
	Cooperation (total)	
	PPML	
Temp>32	0.0501**	0.0475**
	(0.0199)	(0.0190)
Temp 28-32	0.0163	0.0161
	(0.0174)	(0.0168)
Lag Temp>32	0.0378***	0.0273**
	(0.0113)	(0.0131)
Lag Temp 28-32	0.0186**	0.0164
	(0.00892)	(0.0101)
Lag 2 Temp>32		0.0255
		(0.0180)
Lag 2 Temp 28-32		0.0223***
		(0.00861)
Observations	9,542	9,268
Weather Controls	Yes	Yes
City-Month FE	Yes	Yes
City-Year FE	Yes	Yes
Year-Month FE	No	No
Period	Jan 2013-Dec 2015	
Level	City-Year-Month	
Mean of Y	12.76	13.14
SD of Y	39.79	40.31

Notes: The sample covers about 9,800 city-year-month observations (273 cities and 36 months) from January 2013 to December 2015. We employ Poisson Pseudo Maximum Likelihood (PPML) regressions for all columns. Total cooperation is measured by the number of cooperation events. Temperature bins are measured by the monthly number of days with daily mean temperature in the corresponding temperature range. Temperature bin 20-24°C is chosen as the reference bin. Weather controls include precipitation, wind speed, and relative humidity. *** p<0.01, ** p<0.05, * p<0.1. The standard errors are two-way clustered at the city and year levels.

Table 11: Effects on Protests

	(1)	(2)
	Protest (total)	Protest (total)
	PPML	
Temp>32	0.111	0.0192
	(0.0961)	(0.0230)
Temp 28-32	-0.00288	-0.0201
	(0.0319)	(0.0214)
Temp 24-28	0.0243	0.00922
	(0.0191)	(0.0154)
Temp 16-20	0.0279***	-0.0158
	(0.00947)	(0.0236)
Temp 12-16	0.110***	0.00195
	(0.0155)	(0.00460)
Temp 8-12	0.0901**	-0.0330**
	(0.0378)	(0.0144)
Temp 4-8	0.0810***	0.00221
	(0.0298)	(0.00421)
Temp 0-4	0.109***	0.0108
	(0.0353)	(0.0132)
Temp -4-0	0.0743	-0.0152
	(0.0612)	(0.0438)
Temp<-4	0.0742	0.00365
	(0.0748)	(0.0114)
Observations	9,804	9,816
Weather Controls	Yes	Yes
City-Month FE	Yes	No
City-Year FE	Yes	Yes
Year-Month FE	No	Yes
Period	Jan 2013-Dec 2015	
Level	City-Year-Month	
Mean of Y	0.889	0.888
SD of Y	4.349	4.347

Notes: The sample covers about 9,800 city-year-month observations (273 cities and 36 months) from January 2013 to December 2015. We employ Poisson Pseudo Maximum Likelihood (PPML) regressions for all columns. Total cooperation is measured by the number of cooperation events. Temperature bins are measured by the monthly number of days with daily mean temperature in the corresponding temperature range. Temperature bin 20-24°C is chosen as the reference bin. Weather controls include precipitation, wind speed, and relative humidity. *** p<0.01, ** p<0.05, * p<0.1. The standard errors are two-way clustered at the city and year levels.

Table 12: Evaluating the economic impacts of cooperation and climate change

	(1)	(2)	(3)	(4)
		log(GDP)		
		OLS		
Temp>32	-0.00478**			
	(0.00220)			
Temp 28-32	-0.00529***			
	(0.00189)			
log(Cooperation, total)		0.0191**		
		(0.00674)		
log(Cooperation, diplomatic)			0.00233	
			(0.00808)	
log(Cooperation, econ & tech)				0.0153**
				(0.00678)
City FE	Y	Y	Y	Y
Year FE	Y	Y	Y	Y
Observations	1,694	1,694	1,694	1,694
R-squared	0.957	0.956	0.957	0.956

Notes: The sample covers 1,694 city-year observations (273 cities and 6 years) from 2013 to 2018. We employ OLS regressions for all columns. Temperature bins are measured by the yearly number of days with daily mean temperature in the corresponding temperature range. Temperature bin 20-24°C is chosen as the reference bin. We control for city fixed effects and year fixed effects in all columns. *** p<0.01, ** p<0.05, * p<0.1. The Standard errors are clustered at the city and year levels.

Table 13: Effects of policy responses

Change by percentage	5	10	15	20	25	30	35	40	45	50
Subsidize labor	0.275	1.210	1.357	1.878	1.986	2.652	2.759	4.713	5.205	5.424
Subsidize capital	1.280	2.803	4.366	5.755	6.422	7.673	9.118	10.030	12.250	12.442
Subsidize cooperation	1.679	3.461	5.709	6.978	9.468	10.916	11.264	15.539	17.251	17.033

Notes: The effects of policy responses correspond to changing equilibrium objects by a certain percentage. For example, subsidizing the wage rate by 5% increases the equilibrium growth rate by 0.275%. The effects are obtained by using calibrated parameters and equation (11).

Online Appendix For Publication

Appendix A Additional Tables

Table A1: Definition of cooperation

Category	Description	CAMEO Code
Diplomatic	Express support for, commend, approve policy, action, or actor; defend, verbally justify policy, action, or actor; Call on other parties to support the target; Grant diplomatic recognition, initiate diplomatic relations with a state or a government; Express regret or remorse for an action or situation; Express forgiveness, pardon; Ratify, sign, finalize an agreement, treaty	050-057
Economic and technical	Trade relations and other economic exchanges; Voluntary exchanges or sharing of intelligence and other significant information	061, 064
Law	Military exchanges such as joint military games and maneuvers; Cooperation on judicial matters, such as extraditions and war crimes	062, 063

Notes: The definitition is retrieved from Conflict and Mediation Event Observations Event and Actor Codebook. Conflict and Mediation Event Observations (CAMEO) is a framework for coding event data.

Table A2: Summary statistics

	Observations	Mean	SD	Min	Max
Cooperation total	9816	12.411	39.287	0	1245
Cooperation econ & tech	9816	1.633	6.165	0	106
Cooperation law	9816	0.28	2.192	0	106
Cooperation diplomatic	9816	8.87	30.547	0	1101
Protest total	9816	0.888	4.347	0	205
Protest level	9816	0.359	0.955	0	6
Temp>32	9816	0.113	0.954	0	16
Temp 28-32	9816	1.946	5.078	0	31
Temp 24-28	9816	4.437	6.973	0	30
Temp 20-24	9816	5.165	6.831	0	31
Temp 16-20	9816	4.229	5.642	0	30
Temp 12-16	9816	3.518	5.241	0	30
Temp 8-12	9816	3.101	4.769	0	31
Temp 4-8	9816	2.752	4.822	0	28
Temp 0-4	9816	2.063	4.33	0	27
Temp -4-0	9816	1.303	3.411	0	25
Temp<-4	9816	1.791	6.025	0	31
Precipitation	9816	87.07	94.116	0	861.17
Wind speed	9816	2.104	0.584	0.686	5.334
Sunshine	9816	165.39	62.979	6.713	357.73

Notes: Data on public events is obtained from the Global Database of Events, Language, and Tone (GDELT). The sample covers about 9,800 city-year-month observations (273 cities and 36 months) from January 2013 to December 2015. Cooperation total, Cooperation econ & tech, Cooperation law, and Cooperation diplomatic denote the number of total, economic and technical, law, and diplomatic cooperation events, respectively. Protest total denotes the number of total protest events. The protest level denotes the average degree of protest events. Each bin of Temp refers to the number of days with daily mean temperature falling in each specific temperature bin. Precipitation refers to the total volume of precipitation (mm). Wind speed refers to the average wind speed (m/s). Sunshine refers to the total sunshine duration (hour).

Table A3: Log transformations

	(1)	(2)
	log(1+Cooperation)	arcsinh(Cooperation)
	OLS	
Temp>32	0.0617*	0.0756**
	(0.0145)	(0.0172)
Temp 28-32	0.0166	0.0199
	(0.0156)	(0.0189)
Temp 24-28	0.0135	0.0167
	(0.00756)	(0.00911)
Temp 16-20	0.00676	0.00771
	(0.00650)	(0.00771)
Temp 12-16	0.0263	0.0314
	(0.0162)	(0.0195)
Temp 8-12	0.0408	0.0488
	(0.0203)	(0.0243)
Temp 4-8	0.0432	0.0523
	(0.0231)	(0.0282)
Temp 0-4	0.0288	0.0351
	(0.0183)	(0.0221)
Temp -4-0	0.0296	0.0350
	(0.0191)	(0.0231)
Temp<-4	0.0113	0.0129
	(0.0162)	(0.0192)
Observations	9,804	9,804
R-squared	0.781	0.771
Weather Controls	Yes	Yes
City-Month FE	Yes	Yes
City-Year FE	Yes	Yes
Year-Month FE	Yes	Yes
Period	Jan 2013-Dec 2015	
Level	City-Year-Month	
Mean of Y	1.297	1.590
SD of Y	1.445	1.714

Notes: The sample covers about 9,800 city-year-month observations (273 cities and 36 months) from January 2013 to December 2015. We employ OLS regressions for all columns. Total cooperation is measured by the number of cooperation events (with log transformations). Temperature bins are measured by the monthly number of days with daily mean temperature in the corresponding temperature range. Temperature bin 20-24°C is chosen as the reference bin. Weather controls include precipitation, wind speed, and relative humidity. *** p<0.01, ** p<0.05, * p<0.1. The standard errors are two-way clustered at the city and year levels.

Table A4: Alternative ways of standard error clustering

	(1)	(2)	(3)	(4)	(5)	(6)	(7)	(8)
	Cooperation (total)							
	PPML							
Temp>32	0.0507***	0.0176*	0.0507***	0.0176**	0.0507***	0.0176*	0.0507***	0.0176
	(0.0140)	(0.0106)	(0.00964)	(0.00802)	(0.0118)	(0.00990)	(0.0126)	(0.0111)
Temp 28-32	0.0141	0.00875*	0.0141	0.00875**	0.0141	0.00875***	0.0141*	0.00875
	(0.0105)	(0.00507)	(0.0154)	(0.00361)	(0.0169)	(0.00259)	(0.00773)	(0.00599)
Observations	9,804	9,816	9,804	9,816	9,804	9,816	9,804	9,816
Weather Controls	Yes	Yes	Yes	Yes	Yes	Yes	Yes	Yes
City-Month FE	Yes	No	Yes	No	Yes	No	Yes	No
City-Year FE	Yes	Yes	Yes	Yes	Yes	Yes	Yes	Yes
Year-Month FE	No	Yes	No	Yes	No	Yes	No	Yes
Period	Jan 2013-Dec 2015							
Error Level	City	City	Province	Province	Province-Year	Province-Year	Robust	Robust
	City-Year-Month							
Mean of Y	12.43	12.41	12.43	12.41	12.43	12.41	12.43	12.41
SD of Y	39.31	39.29	39.31	39.29	39.31	39.29	39.31	39.29

Notes: The sample covers about 9,800 city-year-month observations (273 cities and 36 months) from January 2013 to December 2015. We employ Poisson Pseudo Maximum Likelihood (PPML) regressions for all columns. Total cooperation is measured by the number of cooperation events. Temperature bins are measured by the monthly number of days with daily mean temperature in the corresponding temperature range. Temperature bin 20-24°C is chosen as the reference bin. Weather controls include precipitation, wind speed, and relative humidity. *** p<0.01, ** p<0.05, * p<0.1.

Table A5: Exclude first and last days in each month

	(1)	(2)
	Cooperation (total)	
	PPML	
Temp>32	0.0521***	0.0188***
	(0.0141)	(0.00504)
Temp 28-32	0.0146	0.00987***
	(0.0155)	(0.00347)
Temp 24-28	0.0117	0.00758***
	(0.0119)	(0.00262)
Temp 16-20	0.0182**	0.00362*
	(0.00919)	(0.00199)
Temp 12-16	0.0475***	0.00897**
	(0.0177)	(0.00400)
Temp 8-12	0.0651**	-0.00959***
	(0.0294)	(0.00258)
Temp 4-8	0.0625*	-0.00259
	(0.0324)	(0.00702)
Temp 0-4	0.0461*	0.00773
	(0.0267)	(0.00662)
Temp -4-0	0.0405**	-0.0159
	(0.0194)	(0.0106)
Temp<-4	0.00301	-0.00912
	(0.0219)	(0.00746)
Observations	9,804	9,816
Weather Controls	Yes	Yes
City-Month FE	Yes	No
City-Year FE	Yes	Yes
Year-Month FE	No	Yes
Period	Jan 2013-Dec 2015	
Level	City-Year-Month	
Mean of Y	11.69	11.67
SD of Y	37.21	37.19

Notes: The sample covers about 9,800 city-year-month observations (273 cities and 36 months) from January 2013 to December 2015. We employ Poisson Pseudo Maximum Likelihood (PPML) regressions for all columns. Total cooperation is measured by the number of cooperation events. Temperature bins are measured by the monthly number of days with daily mean temperature in the corresponding temperature range. Temperature bin 20-24°C is chosen as the reference bin. Weather controls include precipitation, wind speed, and relative humidity. *** p<0.01, ** p<0.05, * p<0.1. The standard errors are two-way clustered at the city and year levels.

Table A6: Results using weekly data

	(1)	(2)	(3)	(4)
	Cooperation (total)			
	PPML			
Temp>32	0.0761	0.0215	0.0587**	0.00234
	(0.0472)	(0.0332)	(0.0239)	(0.0550)
Temp 28-32	0.00668	-0.0199	0.00859	0.0154
	(0.0274)	(0.0185)	(0.0154)	(0.0148)
Observations	48,262	48,262	48,262	48,262
Weather controls	Yes	Yes	Yes	Yes
City FE	No	No	No	Yes
City-Month FE	Yes	Yes	No	No
City-Year FE	Yes	Yes	Yes	No
City-Week FE	Yes	No	No	No
Year-Month-Week FE	No	Yes	Yes	Yes
Period	2013-2015			
Level	Weekly			
Mean of Y	2.524	2.524	2.524	2.524
SD of Y	9.607	9.607	9.607	9.607

Notes: The sample covers about 48,262 city-year-month-week observations (273 cities and 36 months) from January 2013 to December 2015. We employ Poisson Pseudo Maximum Likelihood (PPML) regressions for all columns. Total cooperation is measured by the number of cooperation events. Temperature bins are measured by the weekly number of days with daily mean temperature in the corresponding temperature range. Temperature bin 20-24°C is chosen as the reference bin. Weather controls include precipitation, wind speed, and relative humidity. *** p<0.01, ** p<0.05, * p<0.1. The standard errors are two-way clustered at the city and year-month-week levels.

Table A7: Results using Daily data

	(1)	(2)	(3)	(4)
		Cooperation (total)		
		PPML		
Temp>32	0.390*	0.0992	0.242	0.173
	(0.218)	(0.190)	(0.168)	(0.201)
Temp 28-32	0.0810	0.0103	0.0860	0.0119
	(0.124)	(0.0577)	(0.0544)	(0.0670)
Observations	298,570	298,570	298,570	298,570
Control climate	Yes	Yes	Yes	Yes
City-Year FE	Yes	Yes	Yes	Yes
City-Month FE	Yes	Yes	No	Yes
City-Day FE	Yes	No	No	Yes
Year-Month-Day FE	No	Yes	Yes	Yes
Period		2013-2015		
Level		Daily		
Mean of Y	0.408	0.408	0.408	0.408
SD of Y	2.072	2.072	2.072	2.072

Notes: The sample covers 298,570 city-year-month-day observations (273 cities and 36 months) from January 2013 to December 2015. We employ Poisson Pseudo Maximum Likelihood (PPML) regressions for all columns. Total cooperation is measured by the number of cooperation events. Temperature bins are measured by the indicator of daily mean temperature falling in the corresponding temperature range. Temperature bin 20-24°C is chosen as the reference bin. Weather controls include precipitation, wind speed, and relative humidity. The standard errors are two-way clustered at the city and year-month-day levels. *** p<0.01, ** p<0.05, * p<0.1.

Table A8: Yearly and semi-yearly data

	(1)	(2)
	Cooperation (total)	
	PPML	
Temp>32	0.0502**	0.0480**
	(0.0237)	(0.0232)
Temp 28-32	0.00927	0.0160
	(0.0117)	(0.0115)
Temp 24-28	-0.00834	-0.000758
	(0.00668)	(0.00432)
Temp 16-20	0.0241*	0.0247
	(0.0143)	(0.0155)
Temp 12-16	0.0370**	0.0343*
	(0.0161)	(0.0177)
Temp 8-12	0.00110	0.0113
	(0.00927)	(0.0175)
Temp 4-8	0.00921	0.0153
	(0.0140)	(0.0135)
Temp 0-4	0.0187	0.0142
	(0.0181)	(0.0123)
Temp -4-0	0.0248	0.0221
	(0.0245)	(0.0174)
Temp<-4	0.0163	0.00465
	(0.0350)	(0.0190)
Observations	999	1,998
Weather Controls	Yes	Yes
City FE	Yes	Yes
Year FE	Yes	No
Semi-year FE	No	Yes
Period	2013-2015	
Level	City-Year	City-Semiyear

Notes: The sample covers 273 cities and 2 years (4 semiyears) from January 2013 to December 2015. We employ Poisson Pseudo Maximum Likelihood (PPML) regressions for all columns. Total cooperation is measured by the number of cooperation events. Temperature bins are measured by the yearly or semi-yearly number of days with daily mean temperature in the corresponding temperature range. Temperature bin 20-24℃ is chosen as the reference bin. Weather controls include precipitation, wind speed, and relative humidity. *** p<0.01, ** p<0.05, * p<0.1. The standard errors are two-way clustered at the city and year levels.

Table A9: Model Estimation

	a_{tau}		b_{tau}	
	Estimate	S.E.	Estimate	S.E.
Temp>32	-0.00703	0.00015	0.00513	0.00020
Temp 28-32	-0.00350	0.00005	0.00377	0.00006
Temp 24-28	-0.00081	0.00058	0.00157	0.00051
Temp 16-20	0.00049	0.00004	0.00150	0.00121
Temp 12-16	0.00070	0.00006	0.00135	0.00007
Temp 8-12	0.00106	0.00006	-0.00010	0.00007
Temp 4-8	0.00174	0.00004	0.00113	0.00005
Temp 0-4	0.00260	0.00006	0.00169	0.00007
Temp -4-0	-0.00004	0.00005	0.00029	0.00006
Temp<-4	0.00006	0.00026	0.00015	0.00018

Appendices Not For Online Publication, Available Upon Request

Appendix B A Simple Model of Collective Actions

The models in this section and in Section 6.1 play different roles. The model in this section rationalizes theoretical predictions in the conceptual framework, whereas the model in Section 6.1 builds a framework for quantitative analysis. The model in this section is nested in that in Section 6.1, with some proofs shared in both models.

The model is an adapted version of Guttman (1978). There is a set of agents or individuals $A = \{1, 2, ..., N\}$. Each agent i exerts effort a_i to participate in a collective action (cooperation), in which his contribution x_i is a function of the effort of all agents:

$$x_i = a_i + b(t) \sum_{j \in i} a_j, \tag{B1}$$

where t is the temperature, and $b(t) > 0$ is the matching rate of agents and is a strictly increasing function of the temperature. $b(t)$ captures the nature of collective actions since an agent's contribution is larger when other agents exert more effort. In the case of cooperation, extreme high temperatures induce agents to exert effort collectively to combat the damage. Agent i's payoff π_i has the following form:

$$\pi_i = f_i(x) - cx_i, \tag{B2}$$

, where $x = \sum_i x_i$ is the total contribution, $f(x)$ is a strictly increasing and strictly concave function of x, c is the marginal cost of effort. Therefore, agent i solves the following problem:

$$a_i^* = \arg\max f_i(\sum_i a_i + b(t) \sum_{j \neq i} a_j) - c(a_i + b(t) \sum_{j \neq i} a_j). \tag{B3}$$

The first-order condition is

$$f_i'(x)(1 + (N-1)b(t)) = c. \tag{B4}$$

Consider two comparative statics. The first one is conducted with respect to tem-

perature t. By implicit function theorem, we have

$$f_i^{''}(x)(1+(N-1)b(t))^2 b'(t)\frac{\partial a_i^*}{\partial t} + f_i'(x)(1+(N-1)b(t)) = 0. \tag{B5}$$

Thus,

$$\frac{\partial a_i^*}{\partial t} = -\frac{f_i'(x)(1+(N-1)b(t))}{f_i^{''}(x)(1+(N-1)b(t))^2 b'(t)} > 0. \tag{B6}$$

Therefore, extreme high temperatures foster collective actions, or cooperation, in our case. This conclusion is supported by our empirical results. Second, consider how the effects of temperature vary with opportunity cost, c. Differentiate again with equation (B6), we have

$$\frac{\partial^2 a_i^*}{\partial t \partial c} = -\frac{-f^{'''}(x)(1+(N-1)b(t))^3 b'(t)\frac{\partial a_i^*}{\partial c} + (f_i^{''}(x)(1+(N-1)b(t))^2 b'(t))\frac{\partial a_i^*}{\partial c}}{(f_i^{''}(x)(1+(N-1)b(t))^2 b'(t))^2}. \tag{B7}$$

Here $\frac{\partial a_i^*}{\partial c} < 0$ since from equation (B5) we have

$$\frac{\partial a_i^*}{\partial c} = -\frac{1}{f_i^{''}(x)(1+(N-1)b(t))^2} < 0. \tag{B8}$$

Therefore, with a further restriction that $f''' \geq 0$ or f''' is close to zero, we have

$$\frac{\partial^2 a_i^*}{\partial t \partial c} = -\frac{-f^{'''}(x)(1+(N-1)b(t))^3 b'(t)\frac{\partial a_i^*}{\partial c} + (f_i^{''}(x)(1+(N-1)b(t))^2 b'(t))\frac{\partial a_i^*}{\partial c}}{(f_i^{''}(x)(1+(N-1)b(t))^2 b'(t))^2} < 0. \tag{B9}$$

Therefore, when the opportunity cost is larger, or the relative return of the collective action is lower, the positive partial effect of temperature on effort is less salient. This conclusion is also supported by our empirical results. To summarize, we have the two following predictions.

Prediction B1. *Higher temperatures foster cooperation.*

Prediction B2. *Higher temperatures foster cooperation more when the opportunity cost is smaller or the return is higher.*

The above two predictions are in line with the hypotheses in Section 2.2. They are

also supported by empirical results in Section 5. Specifically, Prediction B1 is consistent with the results in Table 1, and Prediction B2 is consistent with the results in Table 6.

Appendix C Additional Figures and Tables

Figure C1: Time series of the temperature data

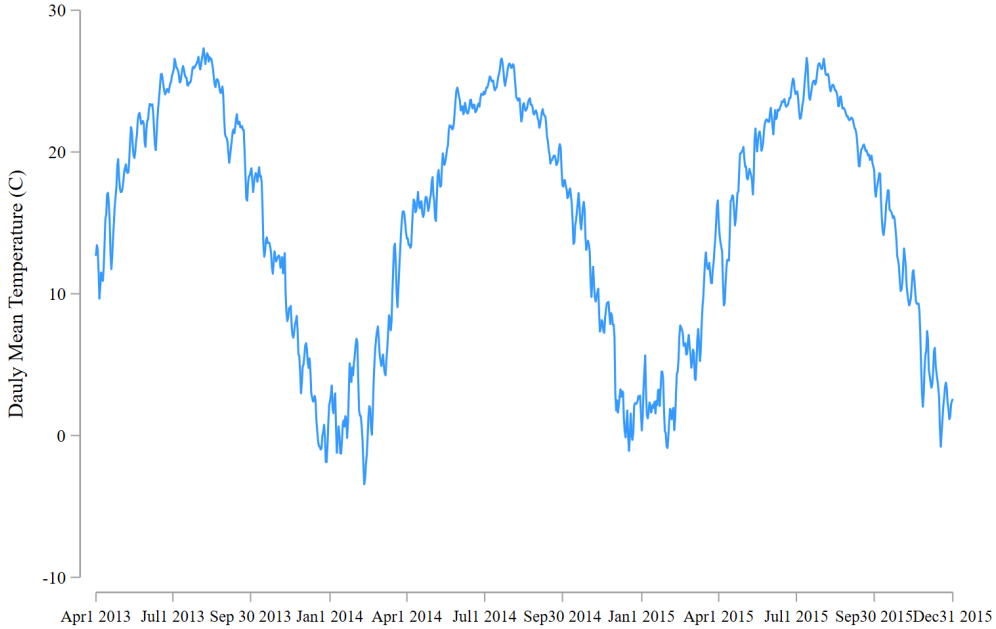

Notes: Figure C1 shows the time series of temperature fluctuations in our sample period.

Figure C2: Map illustration of the temperature data

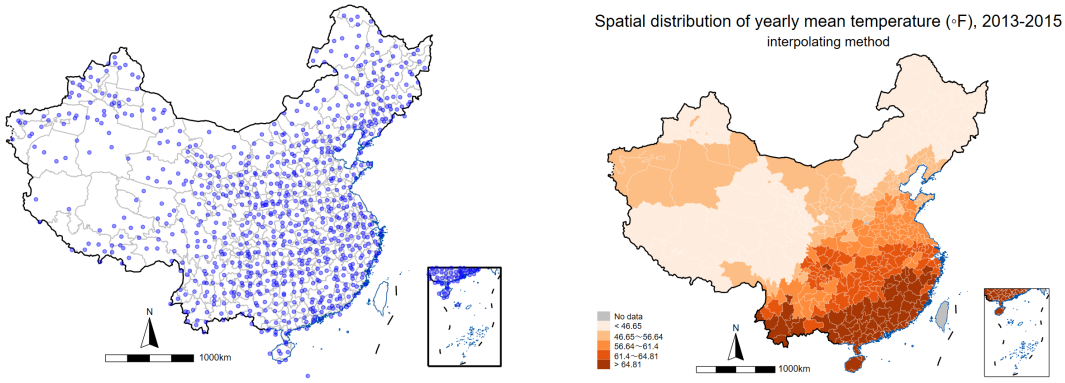

(a) (b)

Notes: Figure C2 (a) shows the spatial distribution of weather stations. Figure C2 (b) shows the spatial distribution of yearly mean temperature, using the interpolating method.

Figure C3: Scatter plots and linear fits

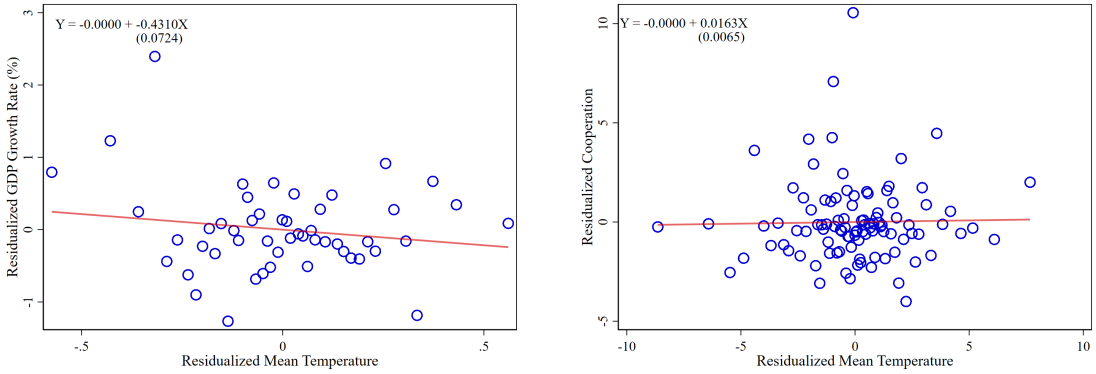

(a) (b)

Notes: Figure C3 (a) shows the relationship between mean temperature and GDP growth. Figure C3 (b) shows the relationship between mean temperature and cooperation.

Table C1: Regional heterogeneity

	(1)	(2)	(3)	(4)	(5)	(6)
	Cooperation (total)					
	PPML					
Temp>32	0.0482**	0.159	0.0449	0.0611	-0.466***	0.174*
	(0.0227)	(0.442)	(0.0298)	(0.681)	(0.0543)	(0.0931)
Temp 28-32	0.00404	-0.0494	0.0793***	0.0452	-0.00863	0.0421
	(0.0313)	(0.0617)	(0.0203)	(0.0643)	(0.0791)	(0.0267)
Temp 24-28	0.00680	-0.00768	0.0192	0.0270	0.0243	0.0373*
	(0.0250)	(0.0259)	(0.0212)	(0.0535)	(0.0198)	(0.0212)
Temp 16-20	0.0373**	0.0407	0.0240	-0.0186	-0.00825	-0.0234
	(0.0171)	(0.0303)	(0.0359)	(0.0588)	(0.0527)	(0.0207)
Temp 12-16	0.0613*	0.0403	0.00346	0.0329	-0.0134	0.0506
	(0.0331)	(0.0636)	(0.0391)	(0.0448)	(0.0520)	(0.0399)
Temp 8-12	0.0415	0.0767	0.0779	-0.0530	0.0322	0.0851*
	(0.0513)	(0.0638)	(0.0872)	(0.0546)	(0.0577)	(0.0487)
Temp 4-8	0.0907	-0.0302	0.0373	-0.0855*	0.0628	0.0865
	(0.0586)	(0.0511)	(0.0634)	(0.0469)	(0.105)	(0.0769)
Temp 0-4	0.0630	0.339**	0.0516	-0.0105	0.103	0.111
	(0.0524)	(0.157)	(0.0875)	(0.0648)	(0.129)	(0.100)
Temp -4-0	0.0922*	0.152	0.0308	0.0125	0.0823	-0.135
	(0.0527)	(0.180)	(0.0777)	(0.0548)	(0.128)	(0.177)
Temp$¡$-4	-0.0836		-0.113**	-0.0469	0.114	-13.20***
	(0.126)		(0.0546)	(0.104)	(0.113)	(0.415)
Observations	2,340	1,260	1,824	1,116	1,116	1,140
Weather Controls	Yes	Yes	Yes	Yes	Yes	Yes
City-Month FE	Yes	Yes	Yes	Yes	Yes	Yes
City-Year FE	Yes	Yes	Yes	Yes	Yes	Yes
Year-Month FE	Yes	Yes	Yes	Yes	Yes	Yes
Period	Jan 2013-Dec 2015					
Region	East	South	Central	North	Northwest	Southwest
Level	City-Year-Month					
Mean of Y	17.50	14.96	10.89	2.973	8.006	11
SD of Y	35.79	44.79	55.65	7.084	20.10	26.76

Notes: The sample covers about 9,800 city-year-month observations (273 cities and 36 months) from January 2013 to December 2015. We employ Poisson Pseudo Maximum Likelihood (PPML) regressions for all columns. Total cooperation is measured by the number of cooperation events. Temperature bins are measured by the monthly number of days with daily mean temperature in the corresponding temperature range. Temperature bin 20-24°C is chosen as the reference bin. Weather controls include precipitation, wind speed, and relative humidity. Some coefficients are not reported due to a lack of variations for identification. *** p<0.01, ** p<0.05, * p<0.1. The standard errors are two-way clustered at the city and year levels.

Table C2: Seasonal heterogeneity

	(1)	(2)	(3)	(4)
	Cooperation (total)			
	Panel A: Drop Spring		Panel B: Drop Summer	
	PPML			
Temp>32	0.0142	0.0129	0.141	-0.451***
	(0.0150)	(0.00814)	(0.566)	(0.167)
Temp 28-32	-0.00182	0.00428	-0.00745	0.0124
	(0.00693)	(0.00411)	(0.0130)	(0.0110)
Observations	7,353	7,362	7,353	7,362
Mean of Y	13.19	13.18	11.99	11.97
SD of Y	41.88	41.86	38.75	38.73
	(5)	(6)	(7)	(8)
	Cooperation (total)			
	Panel C: Drop Fall		Panel D: Drop Winter	
	PPML			
Temp>32	0.113***	0.0129**	0.0519***	0.0213***
	(0.0242)	(0.00630)	(0.0180)	(0.00536)
Temp 28-32	0.0424	0.0146	0.0212	0.00702
	(0.0301)	(0.0112)	(0.0182)	(0.00770)
Observations	7,353	7,362	7,353	7,362
Mean of Y	10.99	10.97	13.54	13.52
SD of Y	33.33	33.31	42.55	42.52
Weather Controls	Yes	Yes	Yes	Yes
City-Month FE	Yes	No	Yes	No
City-Year FE	Yes	Yes	Yes	Yes
Year-Month FE	No	Yes	No	Yes
Period	Jan 2013-Dec 2015			
Level	City-Year-Month			

Notes: The sample covers about 9,800 city-year-month observations (273 cities and 36 months) from January 2013 to December 2015. We employ Poisson Pseudo Maximum Likelihood (PPML) regressions for all columns. Total cooperation is measured by the number of cooperation events. Temperature bins are measured by the monthly number of days with daily mean temperature in the corresponding temperature range. Temperature bin 20-24°C is chosen as the reference bin. Weather controls include precipitation, wind speed, and relative humidity. *** p<0.01, ** p<0.05, * p<0.1. The standard errors are two-way clustered at the city and year levels.

Table C3: Controlling for air pollution

	(1)	(2)
	Cooperation (total)	
	PPML	
Temp>32	0.0981***	0.0147**
	(0.0222)	(0.00629)
Temp 28-32	0.0384*	0.00874
	(0.0204)	(0.00624)
Temp 24-28	0.0358***	0.00860***
	(0.0131)	(0.00197)
Temp 16-20	0.0197	0.00214
	(0.0149)	(0.00363)
Temp 12-16	0.0563***	0.00417
	(0.00795)	(0.00349)
Temp 8-12	0.0671***	-0.00461
	(0.0233)	(0.00529)
Temp 4-8	-0.00109	-0.00754
	(0.0344)	(0.0180)
Temp 0-4	-0.0108	-0.00314
	(0.0353)	(0.0115)
Temp -4-0	-0.0365	-0.0122
	(0.0437)	(0.00841)
Temp<-4	-0.0710	-0.0141
	(0.0460)	(0.0102)
Observations	9,804	9,816
Weather Controls	Yes	Yes
Air Pollution Controls	Yes	Yes
City-Month FE	Yes	No
City-Year FE	Yes	Yes
Year-Month FE	No	Yes
Period	Jan 2013-Dec 2015	
Level	City-Year-Month	

Notes: The sample covers about 9,800 city-year-month observations (273 cities and 36 months) from January 2013 to December 2015. We employ Poisson Pseudo Maximum Likelihood (PPML) regressions for all columns. Total cooperation is measured by the number of cooperation events. Temperature bins are measured by the monthly number of days with daily mean temperature in the corresponding temperature range. Temperature bin 20-24°C is chosen as the reference bin. Weather controls include precipitation, wind speed, and relative humidity. *** p<0.01, ** p<0.05, * p<0.1. The standard errors are two-way clustered at the city and year levels.

Table C4: Daily maximum and minimum temperatures

	(1)	(2)
	Cooperation (total)	
	PPML	
	Daily max	Daily min
Temp>32	0.00787	0.0515***
	(0.0139)	(0.0127)
Temp 28-32	0.00246	0.00929***
	(0.00573)	(0.00341)
Observations	9,816	9,816
Weather Controls	Yes	Yes
City-Month FE	No	No
City-Year FE	Yes	Yes
Year-Month FE	Yes	Yes
Period	Jan 2013-Dec 2015	
Level	City-Year-Month	
Mean of Y	12.41	12.41
SD of Y	39.29	39.29

Notes: The sample covers about 9,800 city-year-month observations (273 cities and 36 months) from January 2013 to December 2015. We employ Poisson Pseudo Maximum Likelihood (PPML) regressions for all columns. Total cooperation is measured by the number of cooperation events. Temperature bins are measured by the monthly number of days with daily max/min temperature in the corresponding temperature range. Temperature bin 20-24°C is chosen as the reference bin. Weather controls include precipitation, wind speed, and relative humidity. *** p<0.01, ** p<0.05, * p<0.1. The standard errors are two-way clustered at the city and year levels.

Table C5: Effects of other climate variables

	(1)	(2)
	Cooperation (total)	
	PPML	
(mean) temperature	0.0117	0.00916
	(0.0243)	(0.00632)
precipitation	0.000512	-4.83e-05
	(0.000831)	(0.000396)
wind speed	-0.00549	0.0101
	(0.0984)	(0.0515)
sunshine duration	0.00233	0.000149
	(0.00148)	(0.000565)
Observations	9,804	9,816
City-Month FE	Yes	No
City-Year FE	Yes	Yes
Year-Month FE	No	Yes
Period	Jan 2013-Dec 2015	
Level	City-Year-Month	
Mean of Y	12.43	12.43
SD of Y	39.31	39.31

Notes: The sample covers about 9,800 city-year-month observations (273 cities and 36 months) from January 2013 to December 2015. We employ Poisson Pseudo Maximum Likelihood (PPML) regressions for all columns. Total cooperation is measured by the number of cooperation events. *** p<0.01, ** p<0.05, * p<0.1. The standard errors are two-way clustered at the city and year levels.

Table C6: Moments comparison

Province	Data moments	Model moments
110000	1489.448	1475.963
120000	32.604	32.908
130000	1.257	1.259
140000	1.353	1.349
150000	0.472	0.472
210000	4.733	4.767
220000	9.831	9.856
230000	0.912	0.917
310000	382.646	381.964
320000	8.280	8.328
330000	9.942	9.998
340000	2.721	2.730
350000	12.728	12.735
360000	2.960	2.951
370000	2.932	2.952
410000	1.963	1.965
420000	8.388	8.389
430000	2.722	2.718
440000	9.039	9.077
450000	0.996	1.005
500000	25.073	25.278
510000	4.541	4.548
520000	1.968	1.961
530000	2.221	2.215
540000	1.920	1.938
610000	2.707	2.723
620000	3.196	3.172
630000	0.626	0.626
640000	1.708	1.711
650000	0.653	0.651

Appendix D Case Studies

In this section, we provide two cases of social cooperation. An important feature of cooperation in the two cases below is that it is often associated with signing contracts that happens indoors. Thus, cooperation is less subject to the influence of extreme high temperatures and creates new economic opportunities.

The first case of cooperation is an appeal for agricultural cooperation with Australia initiated by Shenzhen City, Guangdong Province.[F1] There are more than 100 million people living in Guangdong Province who eat about 12 million tonnes of grains each year. But the total demand for cereal is far greater—about two times as much as the province feeds livestock and for other industrial uses. Therefore, an opportunity to cooperate with Australia arises. The country exports about 26 million tonnes of grain a year, enough to meet the total demand of Guangdong. As a result, Shenzhen City signed a contract of cooperation in the trade and production of cereal and grain products in June 2014.

The second case of cooperation is an appeal for agricultural trade expansion with Russia.[F2] In 2013, Chinese companies exported $2.1 billion in agricultural products to Russia. China is ready to further work with Russia to expand bilateral trade in agricultural products. To be more specific, China is willing to expand its economic and trade relations with Russia and will continue to create the conditions for bilateral cooperation in the energy and agricultural sectors, as well as in the fields of infrastructure and technology. As a result, China signed a cooperative contract with Russia in Beijing in August 2014.

[F1] For a news report, see https://www.smh.com.au/business/china-looks-to-australia-to-satisfy-growing-grain-appetite-20140729-zxx2r.html.

[F2] For a news report, see https://sputnikglobe.com/20140818/China-Ready-to-Expand-Agricultural-Trade-With-Russia-192121328.html.